SSP-Based Land Use Change Scenarios: A Critical Uncertainty in Future Regional Climate Change Projections

Melissa Bukovsky[1,1], Jing Gao[2,2], Linda O. Mearns[1,1], and Brian O'Neill[3,3]

[1]National Center for Atmospheric Research (UCAR)
[2]University of Delaware
[3]Univ of Denver

November 30, 2022

Abstract

To better understand the role projected land-use changes (LUC) may play in future regional climate projections, we assess the combined effects of greenhouse-gas (GHG)-forced climate change and LUCs in regional climate model (RCM) simulations. To do so, we produced RCM simulations that are complementary to the North-American Coordinated Regional Downscaling Experiment (NA-CORDEX) simulations, but with future LUCs that are consistent with particular Shared Socioeconomic Pathways (SSPs) and related to a specific Representative Concentration Pathway (RCP). We examine the state of the climate at the end of the 21st Century with and without two urban and agricultural LUC scenarios that follow SSP3 and SSP5 using the Weather Research and Forecasting model (WRF) forced by one global climate model, the MPI-ESM, under the RCP8.5 scenario. We find that LUCs following different societal trends under the SSPs can significantly affect climate projections in different ways. In regions of significant cropland expansion over previously forested area, projected annual mean temperature increases are diminished by around 0.5-1.0. Across all seasons, where urbanization is high, projected temperature increases are magnified. In particular, summer mean temperature projections are up to 4-5 greater and minimum and maximum temperature projections are increased by 2.5-6, amounts that are on par with the warming due to GHG-forced climate change. Warming is also enhanced in the urban surroundings. Future urbanization also has a large influence on precipitation projections during summer, increasing storm intensity, event length, and the overall amount over urbanized areas, and decreasing precipitation in surrounding areas.

SSP-based land-use change scenarios: a critical uncertainty in future regional climate change projections

Melissa S. Bukovsky[1], Jing Gao[2], Linda O. Mearns[1], Brian C. O'Neill[3]

[1] Regional Integrated Sciences Collective, Computational and Information Systems Laboratory and Research Applications Laboratory, National Center for Atmospheric Research, Boulder, CO 80301, USA

[2] Department of Geography and Spatial Sciences & Data Science Institute, University of Delaware, Newark, DE 19716, USA

[3] Pardee Center for International Futures & Josef Korbel School of International Studies, University of Denver, Denver, CO 80208, USA.

Corresponding author: Melissa S. Bukovsky (bukovsky@ucar.edu)

ORCID iDs:
Bukovsky: https://orcid.org/0000-0001-6415-965X
Gao: https://orcid.org/0000-0003-1778-8909
Mearns: https://orcid.org/0000-0002-2875-5830
O'Neill: https://orcid.org/0000-0001-7505-8897

Author Contributions:
Conceptualization: All authors
Formal Analysis: Bukovsky, Gao
Funding acquisition: Mearns, O'Neill
Investigation: Bukovsky, Gao
Methodology: All authors
Software: Bukovsky, Gao
Visualization: Bukovsky
Writing – original draft: Bukovsky
Writing – review & editing: All authors

Submitted to Earth's Future: 26 August 2020
Revised: 1 February 2021

Key Points

1. Local-to-regional projections of temperature and precipitation change are strongly influenced by urban and agricultural land-use changes.
2. Different shared-socioeconomic-pathway-informed land-use changes produce different responses in future regional climate changes.
3. Urban land expansion has a greater influence on contiguous United States climate change projections than agricultural land expansion.

Abstract

To better understand the role projected land-use changes (LUC) may play in future regional climate projections, we assess the combined effects of greenhouse-gas (GHG)-forced climate change and LUCs in regional climate model (RCM) simulations. To do so, we produced RCM simulations that are complementary to the North-American Coordinated Regional Downscaling Experiment (NA-CORDEX) simulations, but with future LUCs that are consistent with particular Shared Socioeconomic Pathways (SSPs) and related to a specific Representative Concentration Pathway (RCP).

We examine the state of the climate at the end of the 21st Century with and without two urban and agricultural LUC scenarios that follow SSP3 and SSP5 using the Weather Research and Forecasting model (WRF) forced by one global climate model, the MPI-ESM, under the RCP8.5 scenario. We find that LUCs following different societal trends under the SSPs can significantly affect climate projections in different ways.

In regions of significant cropland expansion over previously forested area, projected annual mean temperature increases are diminished by around 0.5-1.0°C. Across all seasons, where urbanization is high, projected temperature increases are magnified. In particular, summer mean temperature projections are up to 4-5°C greater and minimum and maximum temperature projections are increased by 2.5-6°C, amounts that are on par with the warming due to GHG-forced climate change. Warming is also enhanced in the urban surroundings. Future urbanization also has a large influence on precipitation projections during summer, increasing storm intensity, event length, and the overall amount over urbanized areas, and decreasing precipitation in surrounding areas.

Keywords: CORDEX, SSP, land-use change, regional climate

Index terms: 1632 Land cover change, 1637 Regional climate change (4321), 3355 Regional modeling (4316), 3354 Precipitation (1854), 4321 Climate impact (1630, 1637, 1807, 8408)

Plain Language Summary

In many regional climate change studies, projections of future climate conditions are produced assuming the current spatial distribution of different land cover types (e.g. urban, cropland, forest, etc.) will stay the same, even for long-term futures. In doing so, they neglect potential impacts of human land-use changes on regional climate, and miss the opportunity to identify potential land-use strategies that could moderate felt climate change effects. In this study, we model urban and agricultural land-use changes (LUCs) following two pathways with different social and environmental trends throughout the 21st Century, and investigate how the LUCs might affect climate change in North America.

We find that future LUCs can strongly influence projections of temperature and precipitation. Generally, urban land expansion casted a larger impact than agricultural land expansion. In areas where croplands replace forests, the temperature increase caused by greenhouse gas warming is reduced, while in and near future urban areas, the temperature increase caused by greenhouses gas warming is doubled by warming effects from urban land expansion. Meanwhile, urban expansion enhances precipitation over urbanized areas making rainfall events heavier and longer, while precipitation in the surrounding areas is reduced.

1 Introduction

To date, many regional climate model (RCM) or limited-area modeling studies have focused on idealized land-use changes (LUCs), where entire land cover types are removed, added, and/or replaced, to examine their effect on weather, climate, or climate change (e.g. Argüeso et al., 2016; Belušić et al., 2019; Davin et al., 2019; Gálos et al., 2011; Huber et al., 2014; Tölle et al., 2018). Few have gone further into more realistic or societally-informed assessments, and examined the effect of future policy-driven land-use change scenarios and their combined effect on climate change in RCM projections. In one recent example, one of few that we know of, Berkmans et al. (2019) used a European policy-based LUC scenario in an RCM to examine the LUC effect on climate relative to greenhouse-gas (GHG) forced climate change for the near-future, and showed a clear influence of the LUC on temperature. Another, Yilmaz et al. (2019), used ongoing and near future infrastructure projects and their effect on local land-use to examine the influence of expanded irrigation on the upper Euphrates-Tigris basin water budget, finding a large climatological and potentially large societal impact. In some instances, RCM projections have been used to inform climate change impacts assessments including implied land-use changes using integrated assessment models, but have not incorporated the LUC into the RCMs (e.g., Harrison et al., 2019). These existing studies leave a critical gap in the assessment of plausible future LUCs and their effects on future climate in regional simulations.

We attempt to narrow this gap using LUC scenarios that are consistent with different Shared Socioeconomic Pathway (SSPs) in RCM simulations to assess the combined effects of greenhouse-gas-induced climate change and scenario-based anthropogenic LUCs on regional climate projections. More specifically, we examine the influence of the LUCs that underlie the combined SSP+Representative Concentration Pathway (RCP) framework using simulations produced for the North-American branch of the international Coordinated Regional Downscaling Experiment (NA-CORDEX) and complementary simulations produced for this assessment that incorporate SSP-based LUC. We aim to answer the question, "Does inclusion of SSP-based LUCs significantly modulate the RCM projections?", as the answer to this simple question may have broadly relevant implications for future regional modeling efforts, as we will discuss. For this initial effort, we focus on the conterminous United States (CONUS), and projections of near-surface temperature and precipitation, two of the most commonly used variables.

As global model simulations produced for Phase 6 of the Coupled Model Intercomparison Project (CMIP6) as a part of the Scenario Model Intercomparison Project (ScenarioMIP; O'Neill et al., 2016) incorporate SSP-based LUC scenarios related to RCP-based future emissions, exploring the effect of SSP-based LUCs in RCMs is highly relevant for informing future downscaling efforts that make use of ScenarioMIP simulations. This is particularly true for large-scale coordinated efforts like CORDEX, making our effort timely as well. Existing NA-CORDEX simulations hold land surface cover constant at present day conditions, which is typical in most, if not all, existing CORDEX simulations globally, while SSP-consistent projections anticipate potentially substantial changes in anthropogenic land-use amounts and patterns. For example, Gao & O'Neill (2020) found the global total amount of urban land can increase 6 fold by 2100, and economically developed regions (e.g. North America) experience comparable amounts of new urban land development to developing regions. All accentuate the need for investigations like ours.

Understanding the magnitude of the regional climate effects of LUC is additionally important to the SSP+RCP scenarios framework (O'Neill et al., 2019), in particular the assumption that climate model simulations that include a particular land-use scenario are a reasonable representation of climate outcomes in scenarios with the same greenhouse gas forcing but a different land-use scenario (O'Neill et al., 2016). Some results with global climate and land-use models challenge this assumption (Jones et al., 2013) and multi-model experiments are underway to further test it (Lawrence et al., 2016), but in general it is an understudied problem. This work helps address this question, and will help inform thinking about possible needed modifications to the scenarios framework to better account for climate-land-use interactions.

2 Methods

2.1 Description of SSPs and SSP-Consistent Land-Use Changes

We use SSP3: Regional Rivalry (A Rocky Road) and SSP5: Fossil-Fueled Development (Taking the Highway) in this study, because together they span the range of uncertainties in both urban and agricultural land-use in the U.S. over the coming decades. Here, agricultural land includes crop and pasture, but not managed forest. Under SSP3, countries generally focus on domestic issues due to increasing nationalism. Economic development is slow, and countries focus on energy and food security. Population growth is low in industrialized countries but high

in developing countries. As such, the U.S. sees an increase in domestic cropland but low population growth, which translates to low urban land expansion. Under SSP5, the global economy grows quickly driven by material-intensive development and fossil fuel exploitation. Global population growth is low overall compared to many other SSPs, but in the U.S. and other high-income countries, the population grows rapidly under a strong globalized economy. As a result, the U.S. sees a large amount of urban land expansion and a minimal increase in domestic cropland. Pastureland area decreases slightly in both scenarios. For more detail on the SSP narratives see O'Neill et al. (2017).

Interestingly, these two scenarios also provide great contrast in our simulations. Because SSP3 experiences primarily cropland expansion and SSP5 primarily urban land expansion, our simulations can isolate the effects of these two different types of land-use change. Note that our future climate simulations follow RCP8.5 (the RCP that reaches 8.5 W/m^2 by 2100; Moss et al., 2010), and that SSP3 usually does not reach the radiative forcing of RCP8.5 in integrated assessment models, as SSP5 does (Riahi et al., 2017). SSP3 produces a radiative forcing of ~7.2 W/m^2 (with range of 6.7-8.0 W/m^2), whereas SSP5 produces a radiative forcing of ~8.7 W/m^2 (Riahi et al., 2017). Therefore, in this study we use an agricultural land projection from a variant of SSP3 developed to ensure consistency with the radiative forcing levels in RCP8.5. This "High Growth" variant of SSP3 (SSP3HG) includes modestly higher GDP growth that increases emissions and also agricultural land-use relative to SSP3, without changing its basic nature (Ren et al., 2018). The urban land projection is based on the original SSP3; the effect of the higher GDP growth on this low urban land development scenario would be small.

The LUCs consistent with the two SSPs were produced using two land-use models (LUMs). For urban land change, we use a newly-developed empirically-grounded modeling framework (consisting of the Country-Level Urban Buildup Scenario (CLUBS) model and the Spatially-Explicit, Long-term, Empirical City developmenT (SELECT) model (Gao & O'Neill, 2019, 2020)) that produces realistic spatial and temporal patterns for long-term urban land change under different SSPs at a ⅛ degree resolution. For agricultural land change, the projections were produced using a spatially-explicit agricultural land-use model at a ½ degree resolution (Meiyappan et al., 2014, Ren et al., 2018). The agricultural land-use model takes the urban land-use projections as input, and assumes if the two land uses (agricultural vs. urban) compete for the same land, urban land use would win. Both LUMs produce projections of LUC

for the beginning of every decade, decade-by-decade. Each also provides the fraction of a grid box covered by the given land-use type as an end product.

2.2 WRF

This study leverages 25-km resolution Weather Research and Forecasting (WRF; Skamarock et al., 2005) version 3.5.1 model simulations that were produced for NA-CORDEX to save on computational costs (Mearns et al., 2017). Specifically, we use the simulations forced by the Max Planck Institute for Meteorology Earth System Model at Low Resolution (MPI-ESM-LR) GCM that follow the historical and RCP8.5 scenarios. The MPI-ESM-LR atmospheric component has a 1.8653° latitude x 1.875° longitude resolution, a mid-range equilibrium climate sensitivity relative to the full set of Coupled Model Intercomparison Program Phase 5 (CMIP5) simulations, and it provides relatively high quality boundary conditions for WRF (Bukovsky & Mearns, 2020; Rendfrey et al., 2018).

The NA-CORDEX WRF configuration uses the United States Geological Survey (USGS) land-use categories listed in Figure 1. These are used in the Unified Noah land-surface model (LSM) parameterization within WRF. The Noah LSM represents the model's land-atmosphere interface and updates model land-surface variables related to, for instance, sensible and latent heat fluxes (SHF and LHF, respectively), soil temperature and moisture, and runoff while solving the surface energy and water balance per grid cell (e.g., Chen and Dudhia, 2001; Chen et al., 2001; Ek et al., 2003). Each USGS land-use type used in WRF has specific, assigned properties related to albedo, roughness, moisture, etc. Land-use is held constant throughout the entire simulation, and from the historical to the future climate in the NA-CORDEX configuration. The simulation domain with the USGS dominant land-use type for each grid box is shown in Figure 1. It is important to note that in this version of WRF, the Noah LSM only uses the dominant land-use category for each grid box when calculating the surface energy and water balance. This version does not have the ability to take into account multiple land types per grid box given their fractional grid coverage (this is an option in newer versions). Additionally, the urban environment is represented in this configuration of WRF, in the Noah LSM, simply as a type of surface cover with specific assigned properties, like the other land-use types in Figure 1. While these are the WRF settings that are most important in interpreting the results herein, a

full list of parameterizations used and other configuration settings may be found on the NA-CORDEX website or in Supporting Information (SI) Table S1 (Mearns et al., 2017).

In order to assess the combined effects of the RCP8.5 GHG-induced climate change and future anthropogenic land-use changes, complementary simulations with the same WRF configuration as used in NA-CORDEX were produced for 2075-2100 with prescribed LUCs that are consistent with SSP3 and SSP5. Future LUCs for 2090 were prescribed and held constant for the entire 2075-2100 timeslice in the complementary simulations. As the NA-CORDEX simulations are transient simulations that cover 1950-2100, with the RCP scenario forcing starting in 2006, in order to guarantee an identical simulation initiation state, the new simulations were started using a restart file from the original NA-CORDEX simulation, but with modified land-use relevant variables, at July 1, 2073 (allowing a 1.5 year spin-up for the simulation to adjust to the new land-use state, which was removed for analysis).

Herein, the original NA-CORDEX historical (for 1980-2005) and future (for 2075-2100) simulations are referred to as "Hist" and "noLUC", respectively. The complementary future simulations (for 2075-2100) with SSP3- and SSP5-based LUCs applied are referred to as SSP3LUC or SSP5LUC.

2.3 Application of LUC in WRF

Crop, pasture, and urban fractional land-use fields from the historical period LUMs are not the same as their respective USGS/WRF counterparts in magnitude or spatial distribution, and in WRF, crop and pasture are represented by multiple land cover categories. Therefore, future changes in land-use from the LUMs could not be directly applied in WRF. In WRF using the USGS land categories, cropland is represented in categories 2-6 (Figure 1), and pasture, i.e. land that is suitable for grazing, could be seen as types 5, and 7-10. For this study, we applied the LUM changes as absolute fractional LUC deltas (as LUM future minus LUM historical period land cover fractions) to the USGS/WRF fractional land-use fields. The updated fractional fields were used to calculate new dominant land-use fields for the future LUC simulations in a later step. The LUC fractional deltas were added to types 2 or 3 for crop, using type 3 (irrigated crop) if it already existed as the predominant crop type in a grid box; pasture was applied to grassland category 7, and urban was applied to the urban land category 1. Total changes across the domain in the fractional land-use type fields for WRF were then adjusted to be within 5% of

those projected by the LUMs. Next, new dominant land-use category fields, the fields used in WRF, and specifically the Noah land-surface parameterization, were calculated from the adjusted land-use fraction fields. Further details regarding the application of the LUM LUCs in WRF and the motivation behind some of the presented choices can be found in the SI in Text S1. Historical, future, and individual change fields for crop, pasture, and urban land fraction from the LUMs and the modified fractional categories for WRF are also provided in the SI in Figures S1-S3 for reference. Changes to the dominant land category for each grid box in WRF for SSP5LUC and SSP3LUC are shown in Figure 2. Changes in the crop, pasture, and urban fractional fields that were used to calculate those new dominant land-use maps in WRF for SSP5LUC and SSP3LUC are summarized in Figure 3. Additionally, the percent of the total area each land-use field represents over CONUS, as applied in WRF, is given in Table 1a.

Note that LUCs were only applied over the U.S., as plotted in Figure 3, as sub-country level crop and pasture projections could not be produced over the other countries in the domain due to the unavailability of historical crop and pasture data at sub-country level scales at the time of production. Land-use history is used to inform the spatial disaggregation of projections that are initially nation-scale within the LUMs. Therefore, the presentation of our results will focus on CONUS, where the results of the application of LUC on the climate are the most relevant.

2.4 Analysis Methodology

Statistical significance of the climate change projections and the differences across the projections is tested at the 0.1 level using bootstrapping with bias correction and acceleration (Efron & Tibshirani, 1993; von Storch & Zwiers, 1999). Seasonal or annual means for every year within the historical and/or future scenario periods being differenced are pooled together, and from this pool, two lots of x number of years are randomly selected, with replacement, where x equals the number of years in one input period (where the two periods have the same length). The average of each lot is taken, and their difference is calculated. This is repeated 10,000 times to produce a distribution of differences from which the lower- and upper-tail critical values are estimated, bias corrected, and compared to the original difference between the two periods to determine if the original difference is outside of the critical values and, therefore, a significant difference. This method provides an estimate of where the differences are outside of the variability present in the range of years used in the analysis with 90% confidence.

We calculate several precipitation statistics: precipitation intensity, the percent of hours out of all hours that are either wet (%Wet, a.k.a., precipitation frequency) or dry (%Dry), the average number of consecutive wet hours per precipitation event (CWH), and the average number of consecutive dry hours between precipitation events (CDH). Intensity is the average precipitation rate across wet hours only. Wet hours are defined as hours with precipitation greater than or equal to 0.01 mm/hour, and all others are considered dry. All precipitation statistics were calculated from hourly precipitation output.

Additionally, figure 3 indicates urban-rural point pairs that are used for analysis in Section 3. Each pair of points represents an urban point and an eastward (or downwind, at least in winter) rural point (or at least less urban). Urban points in Figure 3 from west-to-east across the domain indicate the Dallas/Fort Worth, TX metroplex (DFW), the Minneapolis/St. Paul, MN metropolitan area (MSP), the Chicago, IL metropolitan area (CHI), the central Florida megaregion centered on Tampa (FL), and the Northeast Megalopolis centered on New Jersey (NJ).

3 Results

3.1 Impact of LUC on Temperature Projections

Mean temperature projections from our MPI-ESM-LR-driven WRF simulations for most of CONUS range from about 3-6°C in the annual mean, 3-7.5°C in winter (December – February; DJF), and 3.5-4.5°C in summer (June-August; JJA) without LUC (Figure 4). Projected increases are greatest in the Upper Midwest, particularly in DJF, and the Interior West, particularly in JJA. Under SSP3LUC, projected warming decreases by 0.25-1.0°C, over a region stretching from the southern Texas-Louisiana border through Arkansas and into Missouri, regardless of season (Figure 4b, e, and h and Figure 5a, d, and g). Similar areas of noticeably cooler projections are also scattered throughout the rest of the Southeast U.S. and occasionally in the Western U.S. under SSP3LUC. These significantly cooler projections are strongly tied to locations where the dominant land-use category at a grid box in WRF changed from a forest type to cropland to accommodate the large increases in cropland in SSP3 (cf. Figure 2a, c, and Figure 5a, d, and g). In JJA, the cooling effect of deforestation is most pronounced where deciduous broadleaf forest was replaced with cropland, and in DJF, where evergreen needleleaf forest was replaced. However, the average cooling effect on the projections over scenario-respective,

dominant-cropland area over CONUS is only -0.18°C in JJA compared to -0.44°C in DJF (Table 1d). Conversely, the scattering of points across the Western U.S. that are 0.25-0.75°C warmer in Figure 5a, d, and g (particularly from Northeast Oregon to Southwest Montana) are coincident with grid boxes that changed from dominantly grassland/pasture to a forest type in WRF due to the decrease in pasture in SSP3. The change in pastureland area, however, is small relative to the changes in cropland and urban land; therefore, the influence of pasture LUC is also small (less than 0.1°C) when considering the mean influence across all CONUS pasture area (Table 1d). The urban land increase in SSP3LUC is also small, and so is its overall effect on temperature (Table 1b and c), but over some urbanized points in Figure 5a, d, and g, projected mean temperatures are around 1-3.5°C warmer than in noLUC.

The most notable and significant differences in the projections from SSP5LUC versus noLUC are the regions of additional warming of 0.5°C up to about 4°C in the annual mean, to 1.5-2.75°C depending on the region in winter, to upwards of 4.5°C in summer (Figure 5b, e, and h). This additional projected warming is strongly tied to areas of urbanization in SSP5, but unlike the most significant changes in SSP3LUC, the additional warming projected in SSP5LUC expands beyond just the grid boxes that change to a dominantly urban land-use category over a greater region, especially in JJA. This is most obvious in the differences that are between 0.25-1.0°C (in light to dark gray) in Figure 5, which surround the areas that have changed to dominantly urban land (cf. Figure 2 and 5b, e, and h). Overall in SSP5LUC, the LUCs, predominantly the larger urbanization effect, increase CONUS mean temperature projections by 0.16°C in DJF and 0.25°C in JJA (Table 1b). Whereas, in SSP3LUC the total LUC effect on CONUS mean temperature projections is only 0.03°C in DJF and -0.02°C in JJA (Table 1b), even though dominant urban land in SSP5LUC accounts for only 3.24% of CONUS land area (a 2.79% increase over Hist and noLUC; Table 1a) and dominant cropland in SSP3LUC accounts for 23.38% of CONUS land area (a 9.26% increase over Hist and noLUC). In the end, CONUS-average projections are warmer in SSP5LUC than in SSP3LUC (Table 1b), and the differences between the scenarios are greatest across the Eastern U.S. (Figure 5c, f, and i). Some of the projection differences noted for SSP3LUC, where the climate change induced warming is decreased, also apply in SSP5LUC, but to a lesser extent, as the LUCs in crop and pasture are less extensive (Figure 5). For instance, a decrease in projected warming is still evident in

SSP5LUC near the Texas-Louisiana border, where cropland has replaced forest as the dominant land-category in WRF.

The differences between the near-surface mean temperature projections from SSP3LUC and noLUC are likely predominantly due to albedo changes and changes in the partitioning of LHF and SHF. These were shown to be the predominant causes of warming due to afforestation in Davin et al. (2019) across an ensemble of 9 RCMs over Europe, that included a few WRF members, and the predominant causes of cooling due to deforestation across seven coupled global atmosphere-land models in de Noblet-Ducoudré et al. (2012) over North America and Eurasia. However, the partitioning of turbulent fluxes within the models in these studies is an important uncertainty source that causes different model responses to LUCs. Nonetheless, here we likely have similarly influential processes from the Texas-Louisiana border region into Missouri, where warming due to GHG-induced climate change is countered by cooling via deforestation for dryland cropland. Notably, cropland has a higher albedo than forest, which promotes cooler daytime temperatures. Additionally, in JJA in particular, maximum temperature (Tmax) is reduced most where the deciduous forest cover is reduced, and this is additionally coincident with where LHF is increased and SHF is decreased, while further south, where needleleaf forest is reduced and the effect on maximum and mean JJA temperature is smaller, SHF is slightly increased and LHF reduced (Figure 6, and SI Figure S4a-c). Surface roughness may also be playing a role in the cooler projections over the deforested land, as minimum temperature (Tmin) is reduced where forest is reduced for cropland as well (Figure 6). This may be because deforested, lower roughness length land cools more than forested land at night as the stable conditions trap more cool air at the surface, whereas the increased turbulence over forest causes more mixing (Lee et al., 2011).

Differences in projected temperatures due to urbanization, particularly in SSP5LUC are also likely predominantly due to albedo differences and changes in the partitioning of turbulent heat fluxes. Urbanization notably lowers albedo and causes increased SHF and decreased LHF, and warmer daytime and nighttime temperatures as a result, as noted in many previous studies of the urban heat island effect (e.g., Arnfield, 2003; Janković & Hebbert, 2012; Masson, 2006) and as seen here (SI Figure S4d-f and Figure 6). Overall, the effect on minimum temperature is larger than the effect on maximum temperature in SSP5LUC, as illustrated in Figure 6 (right column) for DJF and JJA. This was also seen in Argüeso et al. (2014). For either minimum or

maximum temperature in JJA, the additional warming over urban centers due to urbanization alone is on par with the warming due to GHG-induced climate change alone. The same is generally not true in DJF over much of the U.S., except with minimum temperature in FL.

3.2 Impact of LUC on Precipitation Projections

Annual mean precipitation is projected to increase over much of CONUS north of about 40°N and over parts of the Southeast U.S., while drying is projected for the Southwest U.S. and Mexico (Figure 7a). The same pattern generally exists in DJF, but a greater magnitude increase is projected for the north, less drying is projected for the Southwest U.S., and a stronger decrease is projected in Mexico. In summer, precipitation is projected to strongly decrease over parts of the Southwest U.S. and Mexico, and projections for an increase in precipitation are more limited to Northcentral and Northwest CONUS. Although these projections are from one RCM simulation driven by one GCM, they are consistent with the projections from the full collection of GCMs in CMIP5 (Wuebbles et al., 2017), and generally in agreement with the rest of the NA-CORDEX ensemble (Bukovsky & Mearns, 2020). In SSP3LUC, the precipitation projections change only slightly, regardless of season (Figure 7, Figure 8). For instance, the CONUS-average percent increase of 5.41% in JJA and 21.99% in DJF increase by only an additional 0.56% in SSP3LUC in both seasons (Table 1b). However, there are patterns in the projection difference field that do align with land-use changes in JJA that are worth noting. In the Northwest U.S., for instance, projections for increased precipitation in Southern Idaho and westward from there are enhanced in areas of strong irrigated and dryland crop increases in SSP3LUC that occur at the expense of shrubland. Additionally, the widespread region of deforestation for cropland that occurs from the southern Texas-Louisiana border north into Missouri in SSP3LUC has general, insignificant increases in precipitation projected in noLUC in JJA, but in SSP3LUC the projection switches to a general, insignificant decrease in precipitation (Figure 7 g-h, Figure 8g). Although statistically insignificant, the magnitude of this shift (5-15%) is noteworthy and potentially of practical significance since the sign of the projection changed (from an increase to a decrease), and the spatial extent of the effect is widespread (Figure 8g).

The differences between the noLUC precipitation projections and the SSP5LUC projections are stronger and more noteworthy than those that occur between noLUC and

SSP3LUC (Figure 7 and Figure 8), particularly during the summer over the eastern half of CONUS (Figure 8g-i). Significant increases in precipitation occur over areas that experience urbanization under SSP5LUC in the eastern U.S. in JJA, particularly in areas that become dominantly urban (c.f. Figures 2b, 2d, and 8h. Precipitation projections under SSP5LUC are decreased in the surrounding areas in JJA, especially downstream from the urbanized areas. The same does happen under SSP3LUC, but to a much lesser extent given the much smaller increase in urban coverage. On the other hand, over areas of urban expansion on the West Coast (i.e., near San Francisco, Portland, and Seattle), there is a reduction in precipitation in the SSP5LUC scenario in JJA compared to noLUC. Overall, the CONUS mean precipitation change in JJA in SSP5LUC is drier than in SSP3LUC by about 1% in the absolute sense (Table 1b). SSP5LUC is drier than noLUC and SSP3LUC in the CONUS average because of the widespread drying around the urbanized areas, despite having considerably more precipitation over the dominantly urban points in JJA in this scenario (Table 1c). Specifically, JJA precipitation is projected to increase over scenario-relevant dominant urban points by 15.6%, 24.7%, and 31.0% from Hist to noLUC, SSP3LUC, and SSP5LUC, respectively. Considering that LUCs under SSP3LUC are primarily agricultural and SSP5LUC primarily urban, these results suggest that urban land expansion is potentially more influential than cropland expansion on future precipitation patterns in North America.

As the differences between SSP5LUC and noLUC in the JJA precipitation projections over Eastern U.S. urbanized areas are larger than the differences produced by the agricultural LUCs, statistically significant, and would potentially affect many people, the rest of this section will be spent examining these projections further.

Differences in the JJA projections of precipitation characteristics between SSP5LUC and noLUC for a representative sample of points targeting five Eastern U.S. urban areas that vary in size and location (marked in Figure 3) are summarized in Table 2. These differences indicate that the stronger increase in mean precipitation over Eastern U.S. urbanized areas in the future in JJA is associated with, in all locations, a greater increase in precipitation intensity and longer precipitation events (see “Intensity” and “CWH” in Table 2a for the projection differences, or SI Table S2 for the separate noLUC and SSP5LUC projections). Specifically, under SSP5LUC intensity is projected to be about 32% stronger, and events are projected to be about 12% longer, on average, across the five locations. Differences in hourly precipitation frequency projections

are mixed depending on location, with increases in frequency over DFW, FL, and NJ and decreases over CHI and MSP ("%Wet", Table 2a). Precipitation frequency is projected to decrease at all locations under noLUC, but the sign of the precipitation frequency projection switches between the noLUC projections and the SSP5LUC projections in DFW and FL (SI Table S2). Intensity projections in SSP5LUC are also greater than those in noLUC at the "rural" points east of the urbanized areas, but to a much lesser extent than at the "urban" points (12.92% versus 31.90%, respectively, averaged across the locations: Table 2b versus 2a). The rural points under SSP5LUC all have less frequent precipitation than the noLUC scenario though ("%Wet" and "%Dry", Table 2b), meaning that the projection for decreased precipitation frequency in the noLUC scenario for these points decreases further (SI Table S2). Additionally, many of the rural locations have shorter precipitation events under SSP5LUC and a corresponding increase in the number of dry hours between events (Table 2, "CWH" and "CDH").

Similar processes are at play in producing the different summer precipitation projections from the SSP5LUC scenario near Eastern U.S. urban areas versus the noLUC scenario as are seen in observation-based studies and modeling studies (e.g., Argüeso et al., 2016; Bornstein & Lin, 2000; Niyogi et al., 2011; Shepherd, 2005; Shepherd & Burian, 2003; Wu et al., 2019). The warming, potentially aided by the increased surface roughness, over the large urbanized areas in the SSP5LUC simulations compared to the noLUC simulations induces low-level convergence and low-level upward motion (Figure 9a, b). Surface humidity may be lower in the SSP5LUC simulations over the urbanized areas, as expected due to decreased surface evaporation, but the enhanced low-level convergence in the near surface winds leads to increased moisture flux into the urbanized areas (Figure 9c, d). The enhanced surface warming over the urbanized areas also destabilizes the lower atmosphere, as suggested by the lower convective inhibition (Figure 9e). The lifting condensation level and level of free convection are also higher over the heavily urbanized regions, but so too is the boundary layer height, presumably allowing these levels to be reached more often (Figure 9f-h). All of the above translates into enhanced precipitation over all of the urbanized areas in the form of higher intensity storms and storms that persist for longer (Table 2a). It does not translate to more frequent precipitation than in the noLUC future in all cities though, despite a slight diurnal enhancement in the frequency of precipitation in the late-afternoon/early evening in the Eastern U.S. cities examined (SI Figure S5). In the less urbanized surroundings, conditions are made less favorable for precipitation. This is generally best

represented by the stronger low-level divergence of the near-surface winds outside of the heavily urbanized areas and broad areas of increased convective inhibition across the Eastern U.S., that then leads to fewer and often shorter precipitation events. Near coastal regions, the large urbanized areas and their intense heat island effect also interact with and enhance the sea-breeze. In Florida (FL), this effect is strong enough to lead to a much-enhanced and much more diurnally-persistent sea-breeze throughout the future mean JJA diurnal cycle in SSP5LUC (illustrated using near-surface moisture flux in SI Figures S6-S7). This supports enhanced precipitation frequency and intensity throughout most of the FL diurnal cycle (SI Figure S5).

4 Summary and Discussion

Simulations were performed to examine how not including the land-use change that underlies the SSP+RCP framework may affect regional climate model projections of future climate change performed for CORDEX to date, and to answer the broad, but critical question we posed in the introduction: "Does inclusion of SSP-based LUCs significantly modulate the RCM projections?". Focusing on the effects on mean temperature and precipitation for CONUS, we have found that regional climate change projections are sensitive to SSP-based urban and agricultural land-use changes, as evidenced by statistically significant differences in the projections in some regions. We have also shown that the type of land-use change that is assumed matters (i.e. SSP3 vs. SSP5), a conclusion relevant to the scenarios framework.

In regions of significant crop expansion like the Southeast U.S., particularly under SSP3LUC, projected annual mean temperature increases are dampened by 0.5-1.5°C. In localities with large future urbanization projections (SSP5LUC), projected mean temperature increases are substantially magnified in and beyond urban boundaries. Projections for mean temperature are up to 4-5°C greater in JJA in urban centers. This additional warming in summer is on par with the warming due to GHG-forced climate change alone. This is also the case for both minimum and maximum temperature in JJA under SSP5LUC. In SSP5LUC the additional warming is not limited to urban centers. Projected mean and maximum temperature increases are up to around 0.5 °C greater between them in the eastern half of the U.S. in JJA. While regional precipitation is not greatly influenced by land-use change in SSP3LUC, in SSP5LUC over urbanized areas, mean summer precipitation is considerably enhanced, mostly due to an increase in the intensity of the events, but also an increase in the length of the events. This has

potential implications for projections of increased exposure to urban flooding. Precipitation is also suppressed around the urbanized areas in summer.

Overall, the differences between the projections from the SSP-based LUC scenarios suggests that urban land expansion is potentially more influential than cropland expansion on CONUS temperature and precipitation projections, at least under RCP8.5.

These projections, however, only come from one RCM configuration forced by one GCM under one RCP and two future SSPs. They demonstrate that the CORDEX projections can be significantly affected by including LUCs underlying the SSP+RCP framework. However, more research is needed to document the effect RCM+LUC sensitivities and structural uncertainties have on the projections across different LUC scenarios and across different regions.

For example, as we leveraged NA-CORDEX simulations here, and were constrained by the existing WRF configuration, changing some relevant model options may be worth exploring in future studies. For instance, here the urban environment is simply represented by differences in land surface cover properties, and not an urban canopy model. Therefore, the three-dimensional nature of cities is not represented. Using an urban canopy model would likely provide more realistic simulations. Additionally, the land-surface parameterization used had no option for considering sub-grid scale fractional land cover at the time the CORDEX simulations were produced. It does now, and so do other land-surface schemes, so SSP-based fractional LUCs could be applied in future simulations. Considering only the dominant land-use type in a grid box may have caused an under- and/or over-estimation of the effect of the LUC on the projections, depending on the location and LUC type, and it likely also altered the intended amount of LUC applied in WRF relative to that projected by the land-use models (e.g., compare total versus dominant land area in Table 1a). We hope to examine how these modeling choices affected our results in future work. However, results from this study are broadly consistent with observational-based studies and other modeling studies that have examined the role of LUC on climate in terms of their trend and broad physical effect, as discussed previously in the context of the results. Nonetheless, the resolution in this study is also potentially too coarse for some urbanization effects with or without the use of an urban parameterization as well (e.g. the 50-75km downstream influence of the urban canopy on precipitation seen, for instance, in Niyogi et al. (2011)). A higher resolution would also likely provide a better representation of summer precipitation, in particular, regardless of proximity to an urban area. Furthermore, the effect of

urbanization on the precipitation projections here does not include any changes in anthropogenic aerosols and, therefore, does not consider their effect on nucleation. We also do not consider added anthropogenic heat. Likewise, urban land change considers only the expansion of urban extent. An enhanced dataset of changes in urban morphological characteristics would be more realistic, but is not currently available.

Our methods for applying the LUCs in WRF may also warrant additional study. For example, while we tested different methods for applying the crop projections from the LUM to the different crop types in WRF, we did not examine our application of pasture projections with as much scrutiny. In the future we will experiment with applying the changes to other categories that could be considered pasture, not just grassland. Pasture projections in this case though do not have as widespread an effect on climate as the crop and urban projections, as pastureland area change is small.

Ultimately, this work suggests that for a more complete exploration of uncertainty in future regional climate projections, the regional modeling community should consider the land-use changes that underlie the SSP+RCP framework, and not just the GHG concentration scenarios. This is particularly true as the community looks forward to downscaling simulations from CMIP6 ScenarioMIP (O'Neill et al., 2016). Such analyses, however, would require that sub-national land-use change scenarios that are consistent with all relevant SSP+RCP scenarios be available at near the resolution of the models over, preferably, the full region of interest. As there are many different methods in which the LUC can be incorporated into the RCMs and many different ways in which the land surface can be represented in RCMs, additional sensitivity tests should be performed, like those being produced for LUCAS (Davin et al., 2019) in Europe, and groups which undertake LUC incorporation in their projections should fully document their methods. Finally, the international CORDEX community should discuss modeling strategies and methodology for the use of SSP-based LUC scenarios to establish best-practices.

Acknowledgements & Data

The authors would like to thank the modeling teams that contributed to NA-CORDEX (Mearns et al., 2017). Archiving of NA-CORDEX data was funded by the U.S. Department of Defense's Environmental Security Technology Certification Program. NA-CORDEX data is available via na-cordex.org. Derived data that is essential to reproducing the analysis shown

herein that is not publicly available through NA-CORDEX, including the LUC scenario data as applied in WRF, is available via Bukovsky (2021). We also acknowledge high-performance computing support provided by NCAR's Computational and Information Systems Laboratory (Computational And Information Systems Laboratory, 2017), and NCL (Brown et al., 2012). This research was produced as a part of the Framework for Assessing Climate's Energy-Water-Land nexus by Targeted Simulations (FACETS) project, which is supported by the U.S. Department of Energy's Regional and Global Climate Modeling program via grant DE-SC0016438. Additional support was provided by the Regional Climate Uncertainty Program, managed by Dr. Mearns, funded by NSF under the NCAR cooperative agreement. Dr. Mearns was funded by NCAR, which is funded by the NSF.

References

Argüeso, D., Di Luca, A., & Evans, J. P. (2016). Precipitation over urban areas in the western Maritime Continent using a convection-permitting model. *Climate Dynamics*, *47*(3), 1143–1159. https://doi.org/10.1007/s00382-015-2893-6

Argüeso, D., Evans, J. P., Fita, L., & Bormann, K. J. (2014). Temperature response to future urbanization and climate change. *Climate Dynamics*, *42*(7), 2183–2199. https://doi.org/10.1007/s00382-013-1789-6

Arnfield, A. J. (2003). Two decades of urban climate research: a review of turbulence, exchanges of energy and water, and the urban heat island. *International Journal of Climatology*, *23*(1), 1–26. https://doi.org/10.1002/joc.859

Belušić, D., Fuentes-Franco, R., Strandberg, G., & Jukimenko, A. (2019). Afforestation reduces cyclone intensity and precipitation extremes over Europe. *Environmental Research Letters* 14(7), 074009. https://doi.org/10.1088/1748-9326/ab23b2

Berckmans, J., Hamdi, R., & Dendoncker, N. (2019). Bridging the Gap Between Policy-Driven Land Use Changes and Regional Climate Projections. *Journal of Geophysical Research, D: Atmospheres*, *124*(12), 5934–5950. https://doi.org/10.1029/2018JD029207

Bornstein, R., & Lin, Q. (2000). Urban heat islands and summertime convective thunderstorms in Atlanta: three case studies. *Atmospheric Environment*, 34(3), 507–516. https://doi.org/10.1016/s1352-2310(99)00374-x

Brown, D., Brownrigg, R., Haley, M., & Huang, W. (2012). *NCAR Command Language (NCL)*. UCAR/NCAR - Computational and Information Systems Laboratory (CISL). https://doi.org/10.5065/D6WD3XH5

Bukovsky, M. S., & Mearns, L. O. (2020). Regional Climate Change Projections from NA-CORDEX and their Relation to Climate Sensitivity. *Climatic Change*, *Accepted*, In Press. https://doi.org/10.1007/s10584-020-02835-x

Bukovsky, M. S. (2021). Dataset for Bukovsky et al. (2021): "SSP-Based Land Use Change Scenarios: A Critical Uncertainty in Future Regional Climate Change Projections". *NCAR Digital Asset Services Hub, Boulder, CO.* https://doi.org/10.5065/3sw7-jw75

Chen, F. and Dudhia, J., 2001. Coupling an advanced land surface–hydrology model with the Penn State–NCAR MM5 modeling system. Part I: Model implementation and sensitivity. Monthly weather review, 129(4), 569-585. https://doi.org/10.1175/1520-

0493(2001)129<0569:CAALSH>2.0.CO;2

Chen, F., R. Pielke, Sr., and K. Mitchell, 2001: Development and application of land-surface models for mesoscale atmospheric models: Problems and Promises. Observation and Modeling of the Land Surface Hydrological Processes., V. Lakshmi, J. Alberston, and J. Schaake (Editors), American Geophysical Union, 107-135. DOI:10.1029/WS003

Computational And Information Systems Laboratory. (2017). *Cheyenne: SGI ICE XA Cluster*. UCAR/NCAR. https://doi.org/10.5065/D6RX99HX

Davin, E. L., Rechid, D., Breil, M., Cardoso, R. M., Coppola, E., Hoffmann, P., ... & Raffa, M. (2020). Biogeophysical impacts of forestation in Europe: first results from the LUCAS (Land Use and Climate Across Scales) regional climate model intercomparison. Earth System Dynamics, 11(1), 183-200. https://doi.org/10.5194/esd-11-183-2020

de Noblet-Ducoudré, N., Boisier, J.-P., Pitman, A., Bonan, G. B., Brovkin, V., Cruz, F., Delire, C., Gayler, V., van den Hurk, B. J. J. M., Lawrence, P. J., van der Molen, M. K., Müller, C., Reick, C. H., Strengers, B. J., & Voldoire, A. (2012). Determining Robust Impacts of Land-Use-Induced Land Cover Changes on Surface Climate over North America and Eurasia: Results from the First Set of LUCID Experiments. *Journal of Climate*, *25*(9), 3261–3281. https://doi.org/10.1175/JCLI-D-11-00338.1

Efron, B., & Tibshirani, R. (1993). *An introduction to the bootstrap*. Chapman and Hall/CRC.

Ek, M.B., Mitchell, K.E., Lin, Y., Rogers, E., Grunmann, P., Koren, V., Gayno, G. and Tarpley, J.D., 2003. Implementation of Noah land surface model advances in the National Centers for Environmental Prediction operational mesoscale Eta model. Journal of Geophysical Research: Atmospheres, 108(D22). https://doi.org/10.1029/2002JD003296

Gálos, B., Mátyás, C., & Jacob, D. (2011). Regional characteristics of climate change altering effects of afforestation. *Environmental Research Letters*, *6*(4), 044010. https://doi.org/10.1088/1748-9326/6/4/044010

Gao, J., & O'Neill, B. C. (2019). Data-driven spatial modeling of global long-term urban land development: The SELECT model. *Environmental Modelling & Software*, *119*, 458–471. https://doi.org/10.1016/j.envsoft.2019.06.015

Gao, J., & O'Neill, B. C. (2020). Mapping global urban land for the 21st century with data-driven simulations and Shared Socioeconomic Pathways. *Nature Communications*, *11*(1), 2302. https://doi.org/10.1038/s41467-020-15788-7

Harrison, P. A., Dunford, R. W., Holman, I. P., Cojocaru, G., Madsen, M. S., Chen, P.-Y., Pedde, S., & Sandars, D. (2019). Differences between low-end and high-end climate change impacts in Europe across multiple sectors. *Regional Environmental Change*, *19*(3), 695–709. https://doi.org/10.1007/s10113-018-1352-4

Huber, D. B., Mechem, D. B., & Brunsell, N. A. (2014). The Effects of Great Plains Irrigation on the Surface Energy Balance, Regional Circulation, and Precipitation. *Climate*, *2*(2), 103–128. https://doi.org/10.3390/cli2020103

Janković, V., & Hebbert, M. (2012). Hidden climate change--urban meteorology and the scales of real weather. *Climatic Change*, *113*(1), 23–33. https://doi.org/10.1007/s10584-012-0429-1

Jones, A. D., Collins, W. D., Edmonds, J., Torn, M. S., Janetos, A., Calvin, K. V., Thomson, A., Chini, L. P., Mao, J., Shi, X., Thornton, P., Hurtt, G. C., & Wise, M. (2013). Greenhouse Gas Policy Influences Climate via Direct Effects of Land-Use Change. *Journal of Climate*, *26*(11), 3657–3670. https://doi.org/10.1175/JCLI-D-12-00377.1

Lawrence, D. M., Hurtt, G. C., Arneth, A., Brovkin, V., Calvin, K. V., Jones, A. D., Jones, C. D., Lawrence, P. J., de Noblet-Ducoudré, N., Pongratz, J., Seneviratne, S. I., & Shevliakova, E. (2016). The Land Use Model Intercomparison Project (LUMIP) contribution to CMIP6: rationale and experimental design. *Geoscientific Model Development*, *9*(9), 2973–2998. https://doi.org/10.5194/gmd-9-2973-2016

Lee, X., Goulden, M. L., Hollinger, D. Y., Barr, A., Black, T. A., Bohrer, G., Bracho, R., Drake, B., Goldstein, A., Gu, L., Katul, G., Kolb, T., Law, B. E., Margolis, H., Meyers, T., Monson, R., Munger, W., Oren, R., Paw U, K. T., … Zhao, L. (2011). Observed increase in local cooling effect of deforestation at higher latitudes. *Nature*, *479*(7373), 384–387. https://doi.org/10.1038/nature10588

Masson, V. (2006). Urban surface modeling and the meso-scale impact of cities. *Theoretical and Applied Climatology*, *84*(1-3), 35–45. https://doi.org/10.1007/s00704-005-0142-3

Mearns, L. O., McGinnis, S., Korytina, D., Arritt, R., Biner, S., Bukovsky, M., Chang, H. I., Christensen, O., Herzmann, D., Jiao, Y., & Others. (2017). The NA-CORDEX dataset, version 1.0. *NCAR Climate Data Gateway. Boulder (CO): The North American CORDEX Program*, *10*, https://doi.org/10.5065/D6SJ1JCH.

Meiyappan, P., Dalton, M., O'Neill, B. C., & Jain, A. K. (2014). Spatial modeling of agricultural

land use change at global scale. *Ecological Modelling*, *291*, 152–174. https://doi.org/10.1016/j.ecolmodel.2014.07.027

Moss, R. H., Edmonds, J. A., Hibbard, K. A., Manning, M. R., Rose, S. K., van Vuuren, D. P., Carter, T. R., Emori, S., Kainuma, M., Kram, T., Meehl, G. A., Mitchell, J. F. B., Nakicenovic, N., Riahi, K., Smith, S. J., Stouffer, R. J., Thomson, A. M., Weyant, J. P., & Wilbanks, T. J. (2010). The next generation of scenarios for climate change research and assessment. *Nature*, *463*(7282), 747–756. https://doi.org/10.1038/nature08823

Niyogi, D., Pyle, P., Lei, M., Arya, S. P., Kishtawal, C. M., Shepherd, M., Chen, F., & Wolfe, B. (2011). Urban Modification of Thunderstorms: An Observational Storm Climatology and Model Case Study for the Indianapolis Urban Region. *Journal of Applied Meteorology and Climatology*, *50*(5), 1129–1144. https://doi.org/10.1175/2010JAMC1836.1

O'Neill, B. C., Conde, C., Ebi, K., Friedlingstein, P., Fuglestvedt, J., Hasegawa, T., Kok, K., Kriegler, E., Monteith, S., Pichs-Madruga, R., Preston, B., Sillman, J., van Ruijven, B., & van Vuuren, D. (2019). *Forum on Scenarios of Climate and Societal Futures: Meeting Report* (Pardee Center Working Paper 2019.10.04). University of Denver, Denver, CO.

O'Neill, B. C., Kriegler, E., Ebi, K. L., Kemp-Benedict, E., Riahi, K., Rothman, D. S., van Ruijven, B. J., van Vuuren, D. P., Birkmann, J., Kok, K., Levy, M., & Solecki, W. (2017). The roads ahead: Narratives for shared socioeconomic pathways describing world futures in the 21st century. *Global Environmental Change: Human and Policy Dimensions*, *42*, 169–180. https://doi.org/10.1016/j.gloenvcha.2015.01.004

O'Neill, B. C., Tebaldi, C., Van Vuuren, D. P., Eyring, V., Friedlingstein, P., Hurtt, G., Knutti, R., Kriegler, E., Lamarque, J. F., Lowe, J., Meehl, G. A., Moss, R., Riahi, K., & Sanderson, B. M. (2016). *The Scenario Model Intercomparison Project (ScenarioMIP) for CMIP6*. https://doi.org/10.5194/gmd-9-3461-2016

Rendfrey, T., Bukovsky, M. S., & McGinnis, S. (2018). *NA-CORDEX Visualization Collection* [Data set]. UCAR/NCAR. https://doi.org/10.5065/90ZF-H771

Ren, X., Weitzel, M., O'Neill, B. C., Lawrence, P., Meiyappan, P., Levis, S., Balistreri, E. J., & Dalton, M. (2018). Avoided economic impacts of climate change on agriculture: integrating a land surface model (CLM) with a global economic model (iPETS). *Climatic Change*, *146*(3), 517–531. https://doi.org/10.1007/s10584-016-1791-1

Riahi, K., van Vuuren, D. P., Kriegler, E., Edmonds, J., O'Neill, B. C., Fujimori, S., Bauer, N.,

Calvin, K., Dellink, R., Fricko, O., Lutz, W., Popp, A., Cuaresma, J. C., Kc, S., Leimbach, M., Jiang, L., Kram, T., Rao, S., Emmerling, J., … Tavoni, M. (2017). The Shared Socioeconomic Pathways and their energy, land use, and greenhouse gas emissions implications: An overview. *Global Environmental Change: Human and Policy Dimensions*, *42*, 153–168. https://doi.org/10.1016/j.gloenvcha.2016.05.009

Shepherd, J. M. (2005). A Review of Current Investigations of Urban-Induced Rainfall and Recommendations for the Future. *Earth Interactions*, 9(12), 1–27. https://doi.org/10.1175/ei156.1

Shepherd, J. M., & Burian, S. J. (2003). Detection of Urban-Induced Rainfall Anomalies in a Major Coastal City. *Earth Interactions*, *7*, 1–17. https://doi.org/10.1175/1087-3562(2003)007<0001:DOUIRA>2.0.CO;2

Skamarock, W. C., Klemp, J. B., Dudhia, J., Gill, D. O., Barker, D. M., Wang, W., & Powers, J. G. (2005). *A description of the Advanced Research WRF version 2*.

Tölle, M. H., Breil, M., Radtke, K., & Panitz, H.-J. (2018). Sensitivity of European Temperature to Albedo Parameterization in the Regional Climate Model COSMO-CLM Linked to Extreme Land Use Changes. *Frontiers of Environmental Science & Engineering in China*, *6*, 123. https://doi.org/10.3389/fenvs.2018.00123

von Storch, H., & Zwiers, F. W. (1999). *Statistical Analysis in Climate Research*. Cambridge University Press.

Wuebbles, D. J., Fahey, D. W., Hibbard, K. A., Arnold, J. R., DeAngelo, B., Doherty, S., Easterling, D. R., Edmonds, J., Edmonds, T., Hall, T., Hayhoe, K., Huffman, F. M., Horton, R., Huntzinger, D., Jewett, L., Knutson, T., Kopp, R. E., Kossin, J. P., Kunkel, K. E., … Walsh, J. (2017). *Climate Science Special Report: Fourth National Climate Assessment (NCA4), Volume I*. https://lib.dr.iastate.edu/agron_reports/8/

Wu, M., Luo, Y., Chen, F., & Wong, W. K. (2019). Observed Link of Extreme Hourly Precipitation Changes to Urbanization over Coastal South China. *Journal of Applied Meteorology and Climatology*, *58*(8), 1799–1819. https://doi.org/10.1175/JAMC-D-18-0284.1

Yilmaz, Y. A., Sen, O. L., & Turuncoglu, U. U. (2019). Modeling the hydroclimatic effects of local land use and land cover changes on the water budget in the upper Euphrates--Tigris basin. *Journal of Hydrology*, *576*, 596–609. https://doi.org/10.1016/j.jhydrol.2019.06.074

Tables

Table 1. a) percent of CONUS that is classified as a given land-use type from the dominant land-use field and from the fractional land-use fields (labeled "total") for Hist, noLUC, SSP3LUC (SSP3), and SSP5LUC (SSP5). b-e) Mean JJA and DJF projections or projection differences for precipitation (precip, %) and near-surface mean temperature (temp, °C) for CONUS (b) or land areas that are dominantly urban (c), crop (d), or pasture (e). "noLUC-Hist" provides the mean absolute (temp) or percent (precip) change from the historical period to the future noLUC scenario. The other columns provide the absolute differences between the noted projections.

a) % CONUS	Hist & noLUC	SSP3	SSP5
Dominant Urban	0.45	0.65	3.24
Total Urban	0.90	1.58	5.64
Dominant Crop	14.12	23.38	15.21
Total Crop	14.63	32.72	18.28
Dominant Pasture	15.59	14.33	14.86
Total Pasture	15.88	12.68	15.11

b) CONUS	noLUC -Hist	SSP3- noLUC	SSP5- noLUC	SSP5- SSP3
JJA Precip (%)	5.41	0.56	-0.49	-1.05
DJF Precip (%)	21.99	0.56	0.45	-0.11
JJA Temp (°C)	4.38	-0.02	0.25	0.27
DJF Temp (°C)	4.49	0.03	0.16	0.14

c) Urban	noLUC- Hist	SSP3- noLUC	SSP5- noLUC	SSP5- SSP3
JJA Precip (%)	15.60	9.10	15.37	6.27
DJF Precip (%)	28.64	-0.50	-1.51	-1.01
JJA Temp (°C)	4.14	0.79	2.88	2.08
DJF Temp (°C)	4.68	0.38	1.03	0.65

d) Crop	noLUC -Hist	SSP3- noLUC	SSP5- noLUC	SSP5- SSP3
JJA Precip (%)	11.30	-2.19	-3.43	-1.25
DJF Precip (%)	24.54	-1.48	-0.71	0.77
JJA Temp (°C)	4.27	-0.18	0.19	0.37
DJF Temp (°C)	5.28	-0.44	0.09	0.53

e) Pasture	noLUC- Hist	SSP3- noLUC	SSP5- noLUC	SSP5- SSP3
JJA Precip (%)	6.30	-0.54	0.90	-0.73
DJF Precip (%)	19.39	-0.35	0.95	0.13
JJA Temp (°C)	4.62	0.09	0.13	0.09
DJF Temp (°C)	4.17	0.03	0.13	0.05

Table 2. Absolute differences between the SSP5LUC and noLUC projections of JJA-average percent change in different precipitation characteristics for the points indicated in Figure 3 and defined in Section 2.3. a) Points that are directly over the urbanization centers, and b) eastward/downstream points that are more "rural". Precipitation characteristics are defined in Section 2.4.

a) URBAN	Average (%)	Intensity (%)	%Wet (%)	%Dry (%)	CWH (%)	CDH (%)
CHI	25.44	37.26	-3.18	0.79	8.56	16.46
DFW	41.52	17.94	19.10	-2.10	9.76	-14.15
FL	61.60	33.30	23.31	-6.94	28.51	-2.04
MSP	29.04	51.24	-10.74	2.93	3.23	18.80
NJ	24.65	19.74	7.36	-1.57	7.92	-3.69
Average	36.45	31.90	7.17	-1.38	11.59	3.08

b) RURAL	Average (%)	Intensity (%)	%Wet (%)	%Dry (%)	CWH (%)	CDH (%)
CHI	-9.86	21.46	-17.86	4.57	-5.66	27.02
DFW	-0.51	8.68	-6.14	0.69	-0.57	8.64
FL	-15.51	2.16	-15.31	2.99	-3.70	22.17
MSP	-6.62	22.66	-19.19	5.74	-8.65	16.92
NJ	-9.20	9.62	-10.11	1.36	3.25	34.44
Average	-8.34	12.92	-13.72	3.07	-3.07	21.84

Figures

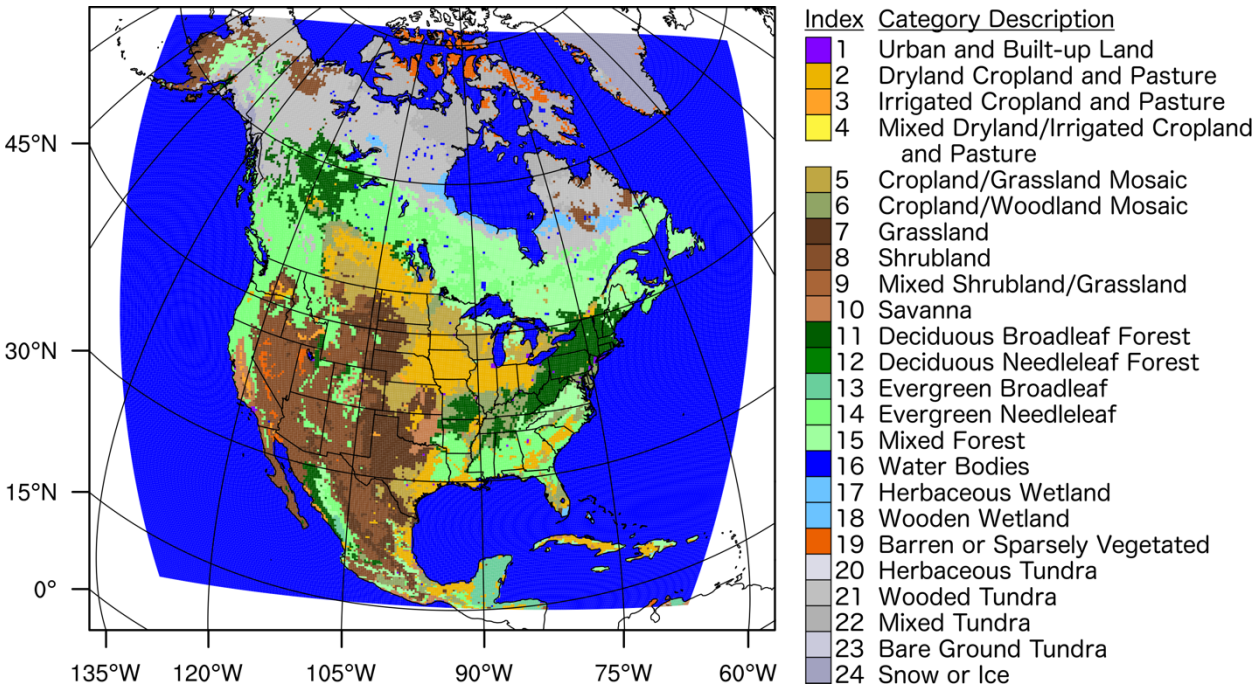

Figure 1. Simulation domain including the dominant land-use category from the baseline simulation for each WRF grid cell. Land-use index with corresponding land-use category description listed on the right.

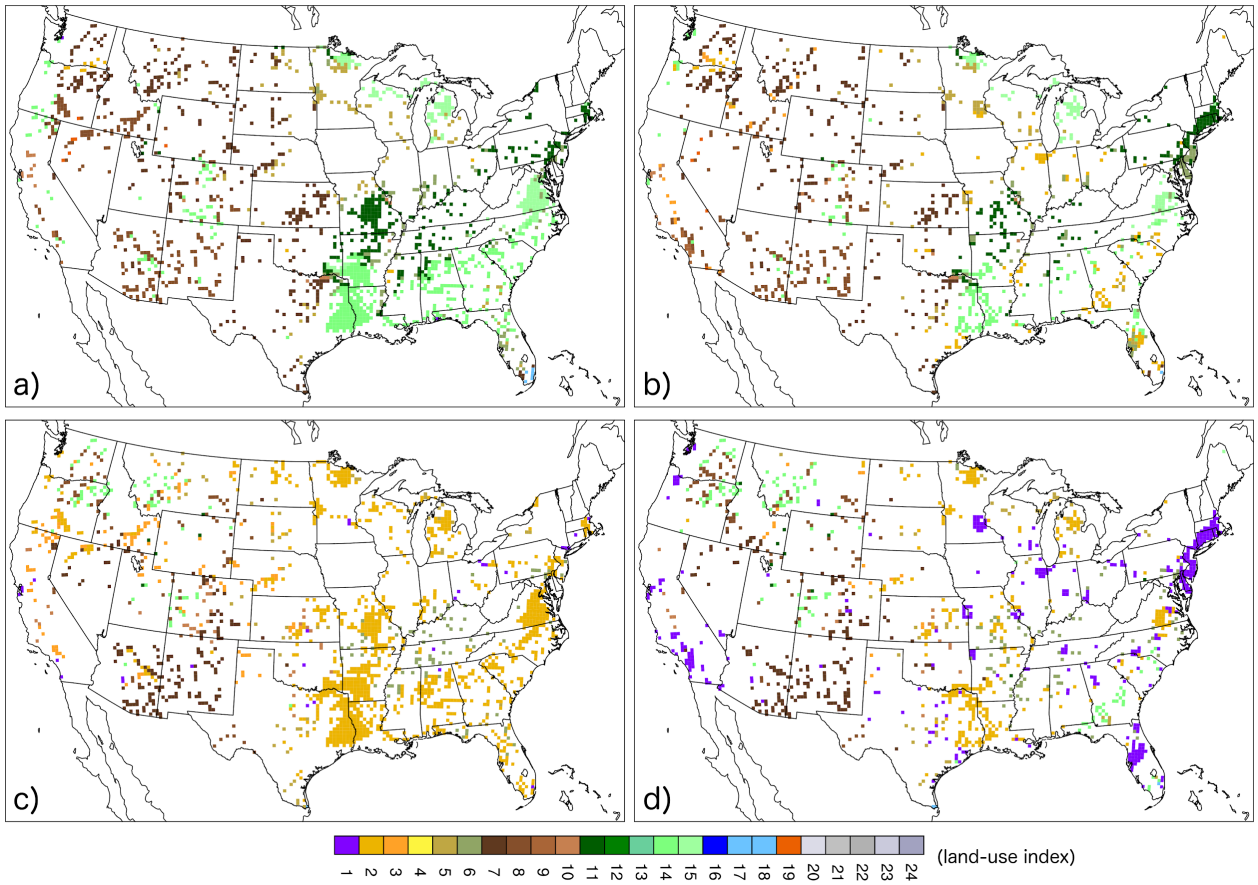

Figure 2. Dominant land-use category for only grid cells that end up changing land-use category under an SSP-based LUC scenario, all others remain white (see Figure 1 for land-use index definition). a) Land-use category used in the Hist and noLUC simulations for cells that change under SSP3LUC; b) as in a), but for cells that change under SSP5LUC; c) new land-use category under SSP3LUC; d) new land-use category under SSP5LUC.

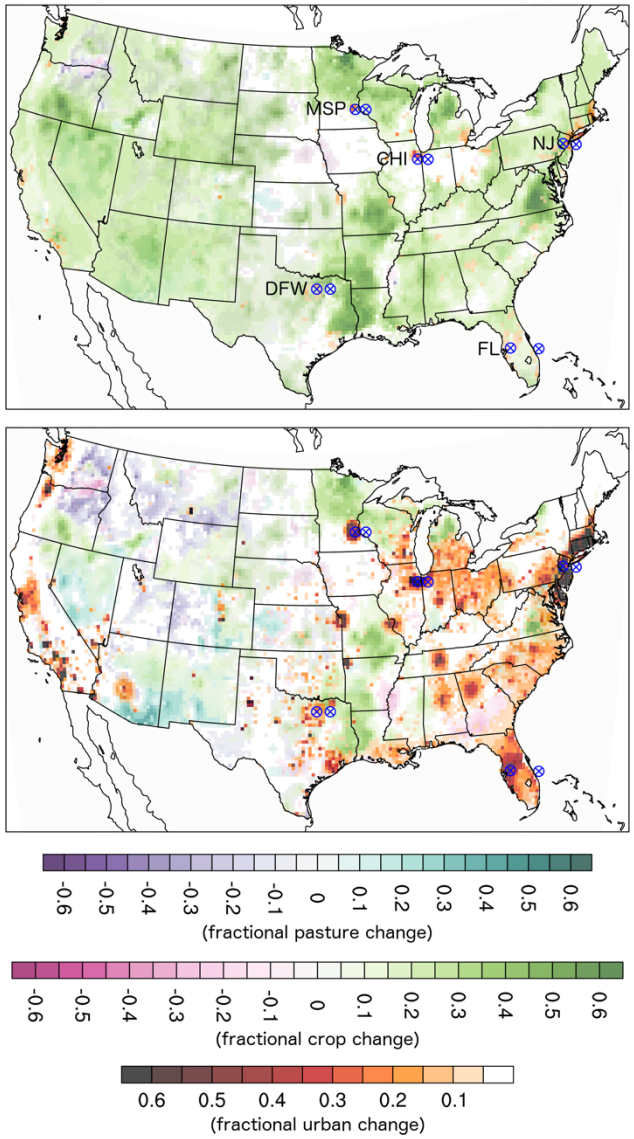

Figure 3. Absolute change in fractional land-use from the baseline to the future in WRF under SSP3LUC (top) and SSP5LUC (bottom). Blue symbols indicate locations of point pairs used in our analysis, as described in Section 2.3. The pair abbreviations are given to the left of each set in the top panel. Fields are plotted at 70% opacity so strong changes in multiple fields at a given point can be identified. Urban change is plotted over crop change, which is plotted over pasture change.

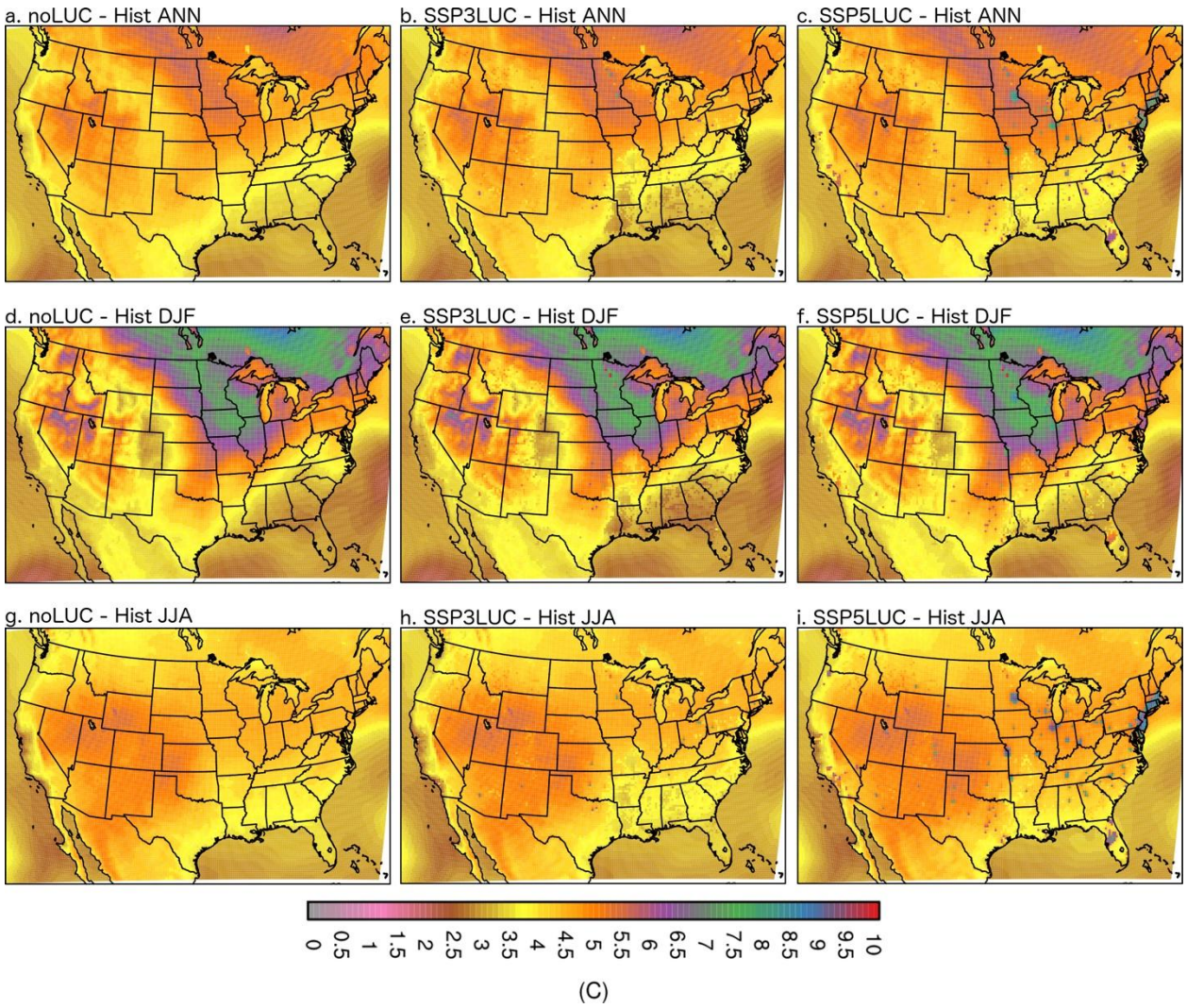

Figure 4. Change in average near-surface mean temperature from 1980-2005 to 2075-2100 for the noLUC future scenario (a, d, and g), the SSP3LUC scenario (g, e, h), and the SSP5LUC scenario (c, f, i) versus Hist. a-c) Annual mean change, d-f) DJF mean change, g-i) JJA mean change. Projections at all points are statistically significant at the 0.1 level, so no indicator of significance was used in this figure.

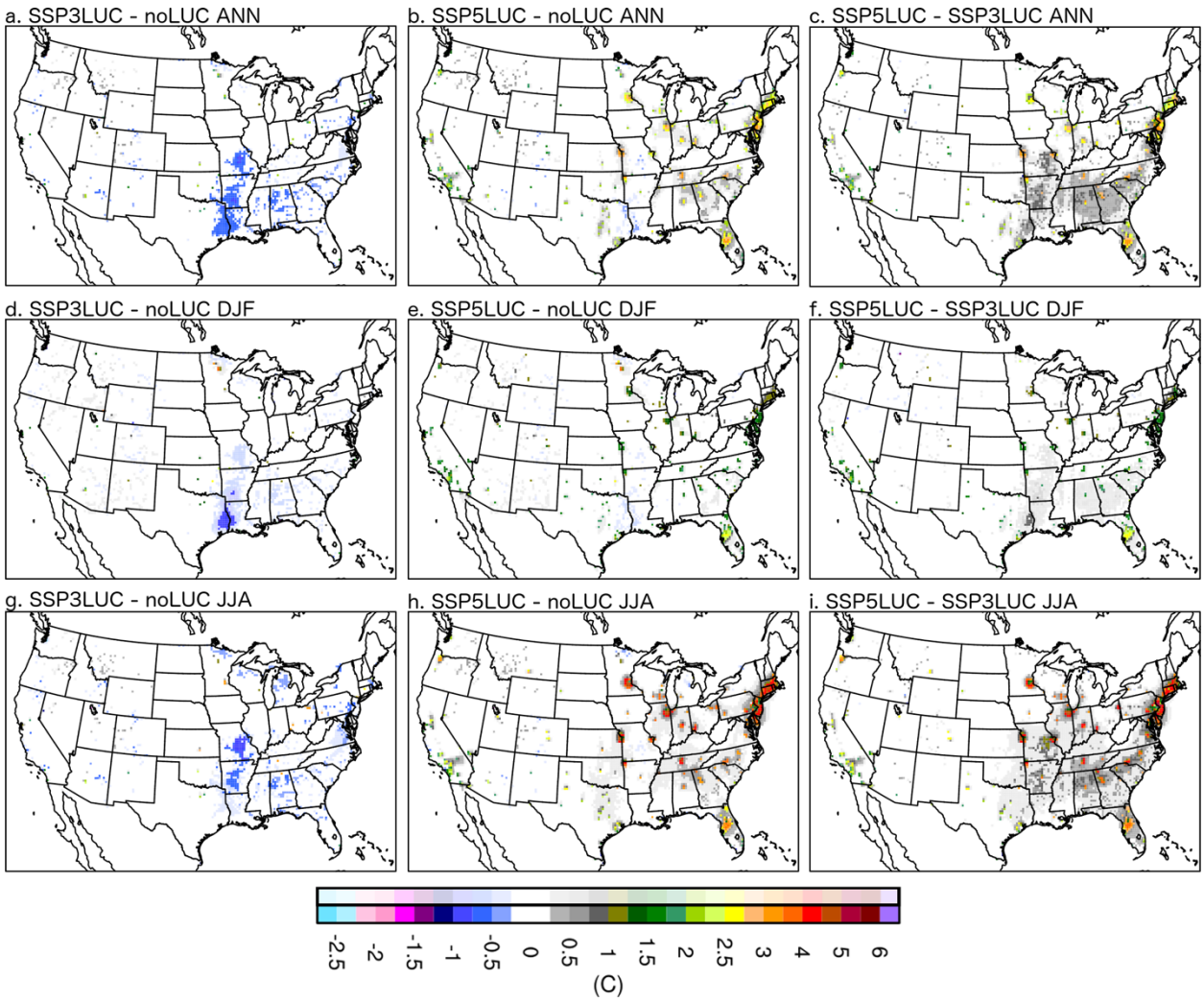

Figure 5. Differences in the average near-surface mean temperature projections across the future scenarios. Left column: SSP3LUC - noLUC, center column: SSP5LUC – noLUC, right column: SSP5LUC – SSP3LUC. a-c) Annual mean difference, d-f) DJF mean difference, g-i) JJA mean difference. Differences that are statistically significant at the 0.1 level follow the lower colorbar, points that are not significant follow the faded upper colorbar.

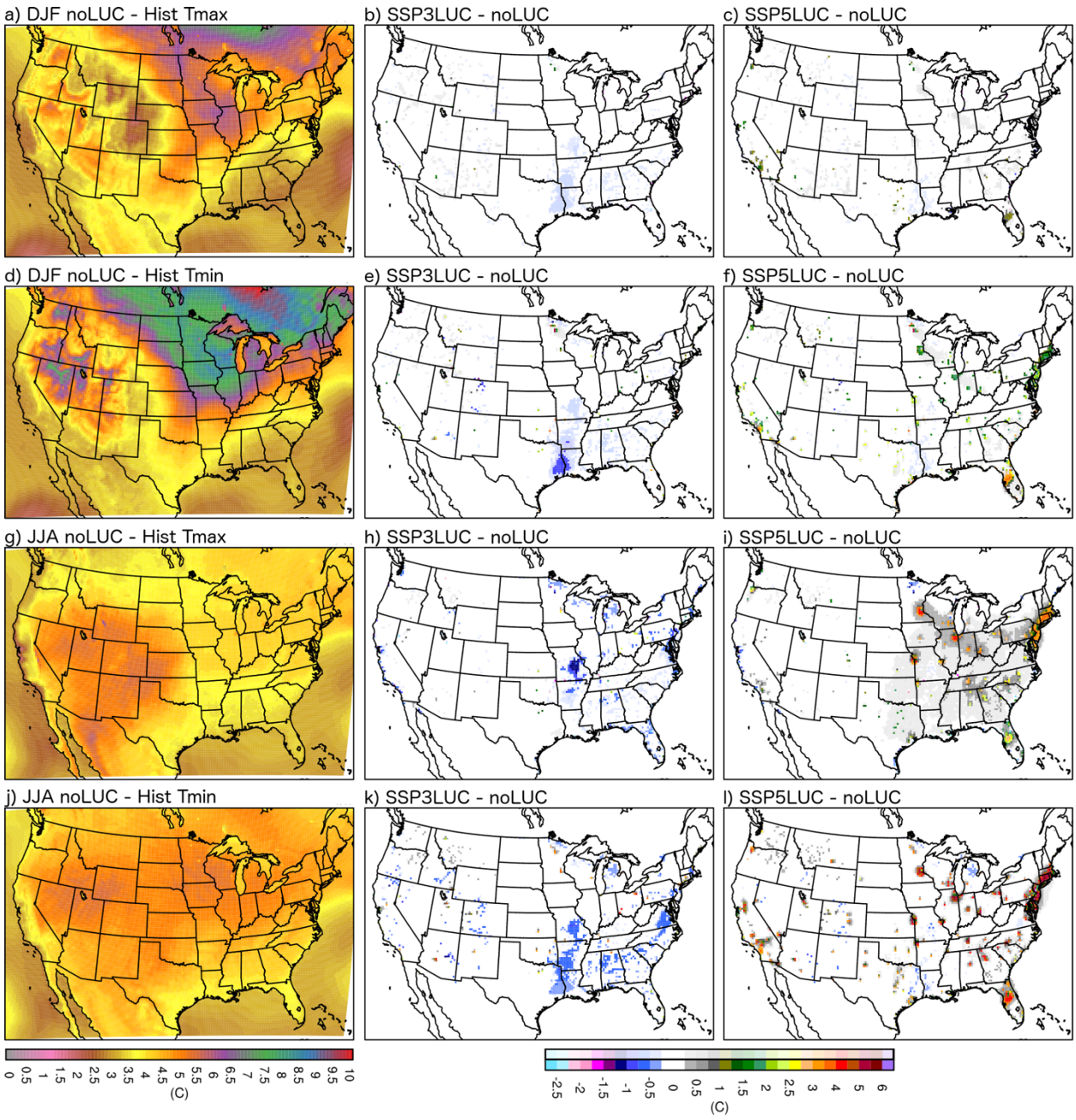

Figure 6. Left column (a, d, g, and j): change in DJF and JJA average Tmax and Tmin from 1980-2005 to 2075-2100 for noLUC versus Hist (as labeled). Projections at all points are statistically significant at the 0.1 level in this column, so no indicator of significance was used. Center column (b, e, h, k): Differences in average Tmax and Tmin projections between the SSP3LUC and noLUC future scenarios. Differences that are statistically significant follow the lower colorbar, points that are not significant follow the faded upper colorbar. Right column (c, f, i, l): as in the center column, but for the SSP5LUC versus noLUC. a-c) DJF Tmax; d-f) DJF Tmin; g-i) JJA Tmax; j-l) JJA Tmin.

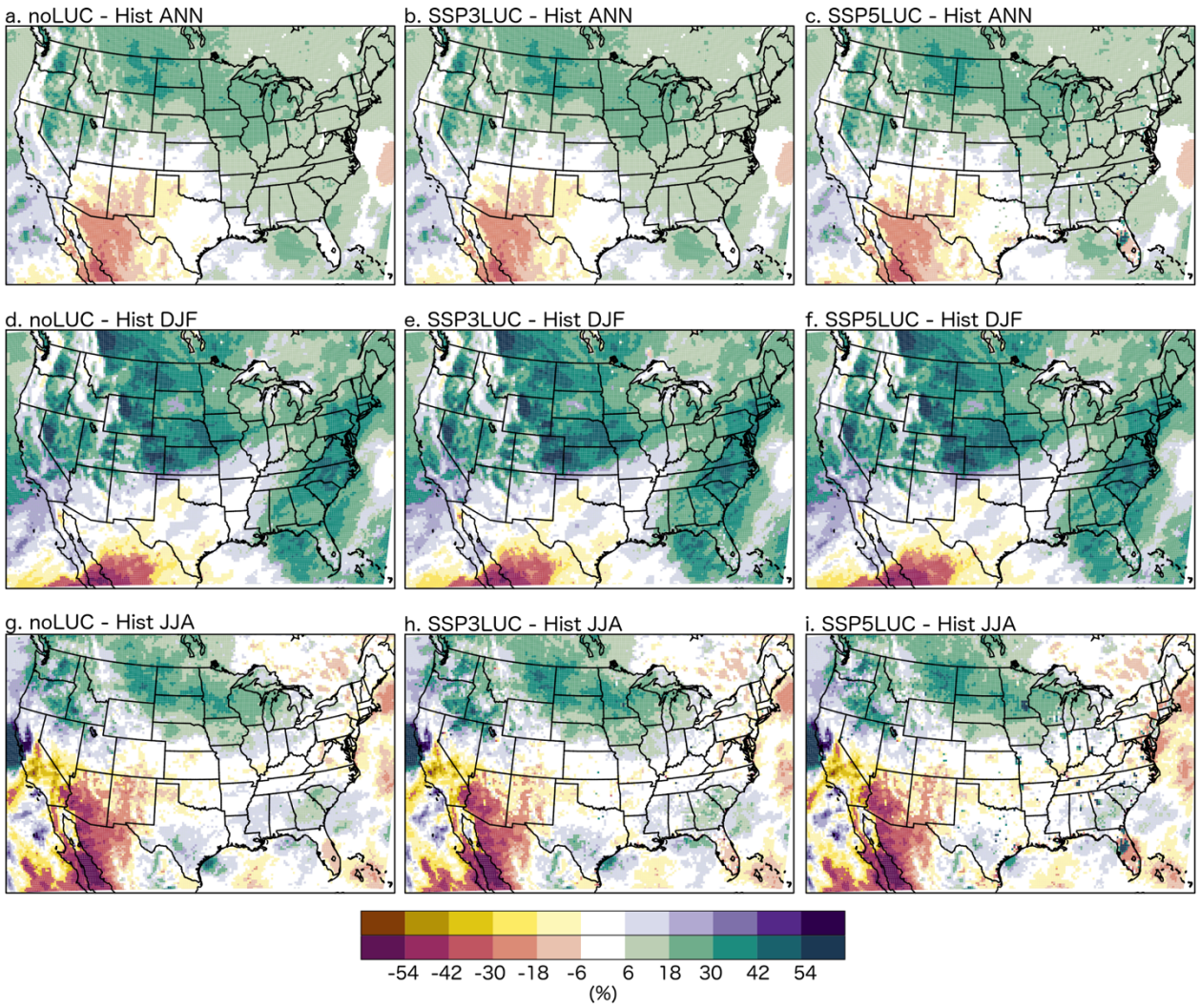

Figure 7. As in Figure 4, but for the percent change in mean precipitation from 1980-2005 to 2075-2100. Differences that are statistically significant at the 0.1 level follow the lower colorbar, points that are not significant follow the upper colorbar.

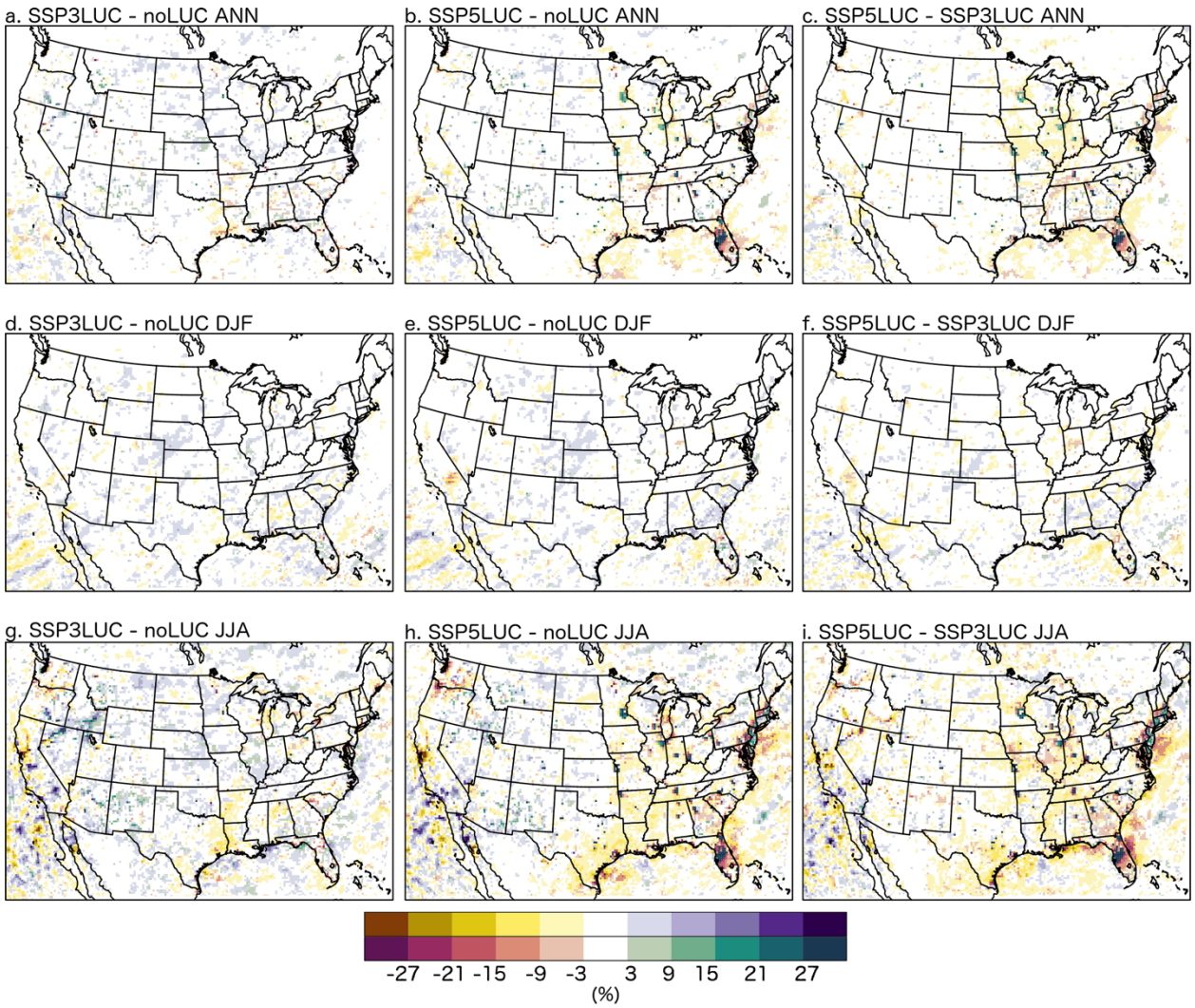

Figure 8. As in Figure 5, but for the absolute difference in the average precipitation percent change projections. Differences that are statistically significant at the 0.1 level *and* grid cells where the significance changed between the projections follow the lower colorbar, points that are not significant follow the upper colorbar.

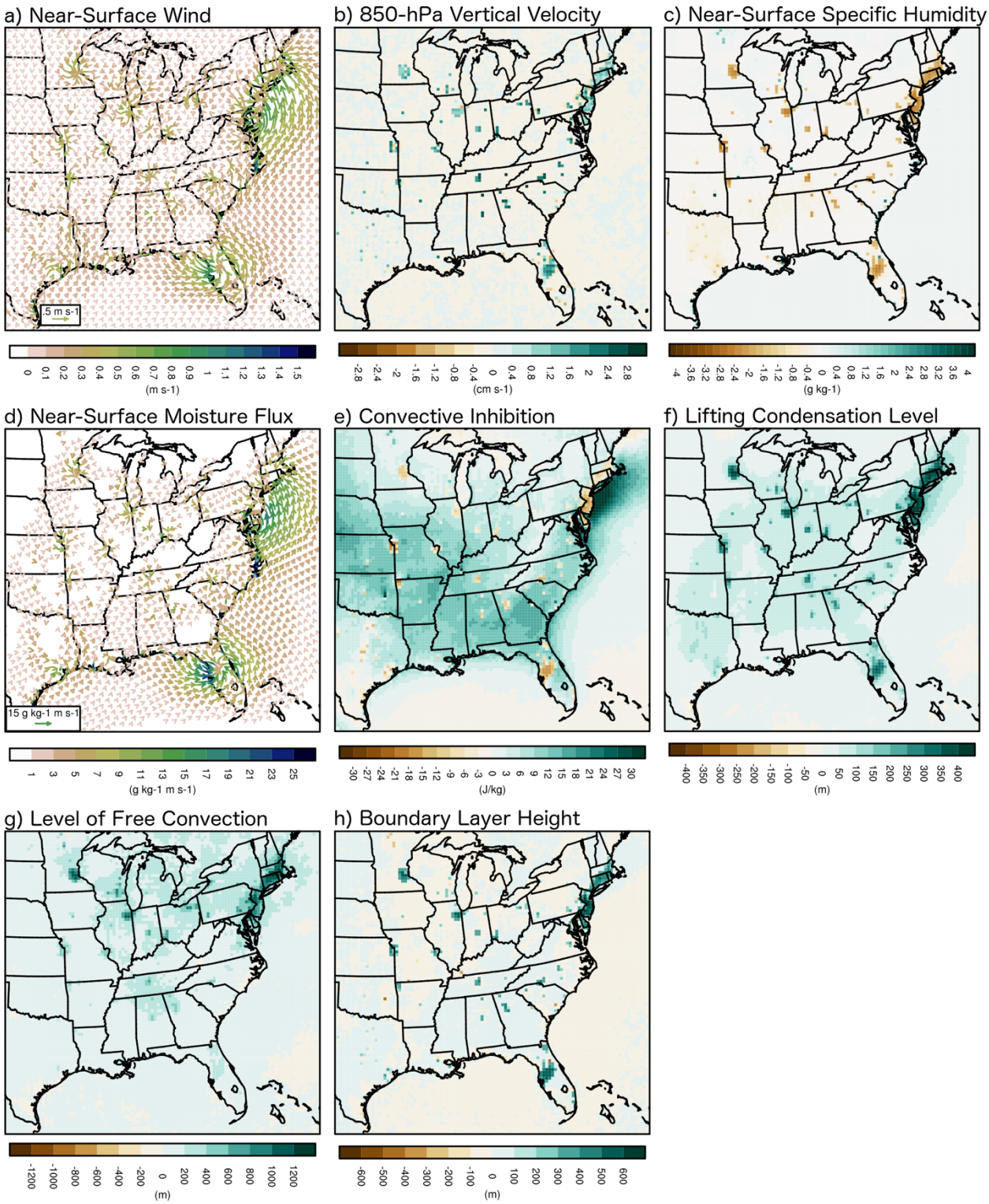

Figure 9. JJA absolute difference between projections from the SSP5LUC and noLUC future scenarios for a) near-surface wind, b) 850-hPa vertical velocity, c) near-surface specific humidity, d) near-surface moisture flux, e) convective inhibition, f) lifting condensation level, g) level of free convection, h) boundary layer height.

Earth's Future

Supporting Information for

SSP-Based Land Use Change Scenarios: A Critical Uncertainty in Future Regional Climate Change Projections

Melissa S. Bukovsky[1], Jing Gao[2], Linda O. Mearns[1], Brian C. O'Neill[3]

[1]Regional Integrated Sciences Collective, Computational and Information Systems Laboratory and Research Applications Laboratory, National Center for Atmospheric Research, Boulder, CO 80301, USA

[2]Department of Geography and Spatial Sciences & Data Science Institute, University of Delaware, Newark, DE 19716, USA

[3]Pardee Center for International Futures & Josef Korbel School of International Studies, University of Denver, Denver, CO 80208, USA.

Contents of this file

Introduction

This Supplementary Information file contains additional methodology information and supplemental figures and tables.

Text S1. Additional Details Related to the Application of LUCs in WRF

Multiple different delta-type methods for incorporating the LUCs into WRF were tested, within the timeframe allowed by the project. We took into consideration which option produced land-use changes in WRF that were most consistent with what was produced in the LUMs, which combination of WRF land-cover types in the historical climate simulations were spatially most consistent with those from the LUMs, which option made sense to the authors in terms of potential scenario storylines, and which could also be applied to other land-cover dataset options with different land-use categories available in WRF (e.g., MODIS).

As the LUM data do not have the same resolution as WRF, the LUM data were first bilinearly interpolated to the 25-km grid used in WRF. Then, absolute fractional LUC deltas (LUM future minus historical period land cover fraction) were applied to WRF USGS fractional land-use fields. We did not use percent deltas, as they produced LUC fields in WRF that were not consistent with the LUM change fields.

LUM crop change deltas were applied to crop categories 2 and 3 in WRF, non-mixed-type dryland and irrigated crop, respectively, depending on which one was already prevalent in a grid box. Dryland crop was modified if no crop type 2 or 3 was present in the original/historical field. LUM pasture changes were applied to land category 7, grassland, in WRF, and urban changes were applied directly to the urban land category 1. Other fractional land-types in a grid box were increased or decreased proportionally to account for the changes in crop, pasture, and urban land. After the absolute crop and pasture change deltas were applied in WRF, the fields were adjusted by adding or subtracting small uniform values from all crop/pasture points until the changes across the domain in WRF in crop and pasture were within 5% of those projected by the LUM. Urban land and water (category 16) fractions were not allowed to change during the application of crop and pasture changes. Urban LUM change deltas were then applied, and considered to be the dominant changes during the land-use field modification process (i.e. they took precedence over any crop/pasture change at a point). Water fractions were not allowed to change in this step either. Finally, the resulting future land-use fraction fields for WRF were used to produce an updated dominant land-use category field for WRF.

We chose to apply the LUC deltas to cropland categories 2 and 3 instead of just to category 2, or to whichever cropland category between 2-6 was most prevalent in a grid box

already for several reasons. First, adding land to categories 2 or 3, instead of the mixed cropland types 4-6, seemed likely to produce a larger climate change signal, and, as a result, allow us to more easily see how much the LUCs could matter to the future climate. In the Southeast U.S., for example, applying the LUC to whichever cropland category was already most prevalent at a point would have meant that many (roughly half) of the points that changed from dominantly forest to dominantly dryland cropland using our chosen method would have changed to mixed cropland/woodland category 6 instead (not shown). This may have made the LUC climate signal smaller and, therefore, harder to separate from the green-house gas induced climate change signal. Applying crop change to only category 2, and ignoring category 3 if it was present at a point, may have produced a similarly larger effect, but it would not have been consistent with observed historical practices. However, if we wanted to use a similar methodology in WRF if the MODIS land-use categories were used instead of the USGS categories, applying LUC to category 2 only would have made this method more transferable, as there is no irrigated cropland category in MODIS. We decided against greater transferability, and for the methodology that would be somewhat more consistent with historical practices. (While cropland is represented in USGS land-use categories 2-6, with categories 4-6 being mixed cropland types, in MODIS, cropland is only represented in 2 categories: a pure "Croplands" category, and a mixed cropland category. In the WRF vegetation and land-use parameter tables, the "Croplands" category is identical to the USGS dryland cropland category 2, meaning that they share set characteristics like albedo, emissivity, and soil moisture availability.)

While pastureland could also be seen as multiple USGS land-use categories, for simplicity we chose to only change category 7, grassland. Pastureland area change is small relative to the SSP3LUC cropland and SSP5LUC urban land area changes, particularly in the dominant land-use category field, so we suspect that this choice had little overall effect on any of our CONUS-to-regional-scale climate change results (although it would matter at the grid-box level). Under a scenario with more pastureland change, or over a part of the world with more pastureland change, we would suggest exploring other options.

Table S1. WRF Configuration. See WRF User's Guide version 3.5 for details and parameter definitions (https://www2.mmm.ucar.edu/wrf/users/docs/user_guide_V3/contents.html). Where relevant, parameterization option number is given in parentheses after the parameterization's name.

Version	3.5.1
Dynamics	Nonhydrostatic, compressible
Sea Ice Characteristics	Fractional sea ice as a lower boundary condition from GCM
Lake Characteristics	Default interpolation from nearby ocean SSTs
Surface Layer	Eta similarity (2)
Boundary Layer	Mellor-Yamada-Janjic Scheme (2)
Land Surface Model	Noah Land Surface Model (2)
Microphysics	WRF Single-Moment 3-Class Scheme (3)
Cumulus Parameterization	Kain-Fritsch Scheme (1)
Longwave Radiation	Rapid Radiative Transfer Model (1)
Shortwave Radiation	Goddard Shortwave (2)
Spectral Nudging	Yes; wind, temperature, and geopotential nudged above layer 10
Top Wave Number to Nudge	7; wavelengths approximately 1000km and longer
Lateral Boundary Treatment	Linear relaxation
Sponge Zone Depth	5
Timestep (seconds)	150
Model Top (hPa)	50
Number of Vertical Levels	28
Surface Input Source	1 (historical and noLUC), 3 (SSP-based LUC scenarios)

Table. S2 Percent change from Hist to the noLUC or SSP5LUC future scenarios (as noted) in JJA-average precipitation characteristics for the points indicated in Figure 3 and defined in Section 2.3. a) Points that are directly over the urbanization centers, and b) eastward/downstream points that are more "rural". Precipitation characteristics are defined in Section 2.4.

a) Urban	Average (%)	Intensity (%)	%Wet (%)	%Dry (%)	CWH (%)	CDH (%)
CHI noLUC	6.23	28.69	-17.44	4.35	-14.45	7.96
CHI SSP5LUC	31.67	65.95	-20.63	5.15	-5.90	24.42
DFW noLUC	1.18	21.17	-16.49	1.81	-4.50	16.55
DFW SSP5LUC	42.70	39.11	2.60	-0.29	5.26	2.40
FL noLUC	-7.61	3.33	-10.59	3.15	-11.95	1.53
FL SSP5LUC	53.99	36.63	12.72	-3.79	16.56	-0.51
MSP noLUC	29.87	35.42	-4.09	1.11	-11.06	-6.22
MSP SSP5LUC	58.91	86.66	-14.83	4.04	-7.83	12.58
NJ noLUC	-10.93	26.55	-29.61	6.30	-12.21	32.56
NJ SSP5LUC	13.72	46.29	-22.24	4.73	-4.29	28.87
noLUC Average	3.75	23.03	-15.64	3.35	-10.83	10.48
SSP5LUC Average	40.20	54.93	-8.48	1.97	0.76	13.55

b) Rural	Average (%)	Intensity (%)	%Wet (%)	%Dry (%)	CWH (%)	CDH (%)
CHI noLUC	9.13	32.58	-17.68	4.52	-13.33	9.84
CHI SSP5LUC	-0.73	54.04	-35.54	9.09	-18.99	36.85
DFW noLUC	0.25	18.80	-15.61	1.77	-9.21	9.53
DFW SSP5LUC	-0.26	27.48	-21.75	2.46	-9.78	18.17
FL noLUC	-2.57	11.46	-12.57	2.45	-4.97	11.27
FL SSP5LUC	-18.07	13.62	-27.88	5.44	-8.66	33.45
MSP noLUC	26.85	28.44	-1.23	0.37	-10.28	-8.83
MSP SSP5LUC	20.22	51.11	-20.42	6.11	-18.93	8.09
NJ noLUC	-5.87	43.59	-34.43	4.64	-10.47	42.87
NJ SSP5LUC	-15.07	53.21	-44.54	6.01	-7.21	77.30
noLUC Average	5.56	26.98	-16.31	2.75	-9.65	12.93
SSP5LUC Average	-2.78	39.89	-30.03	5.82	-12.72	34.77

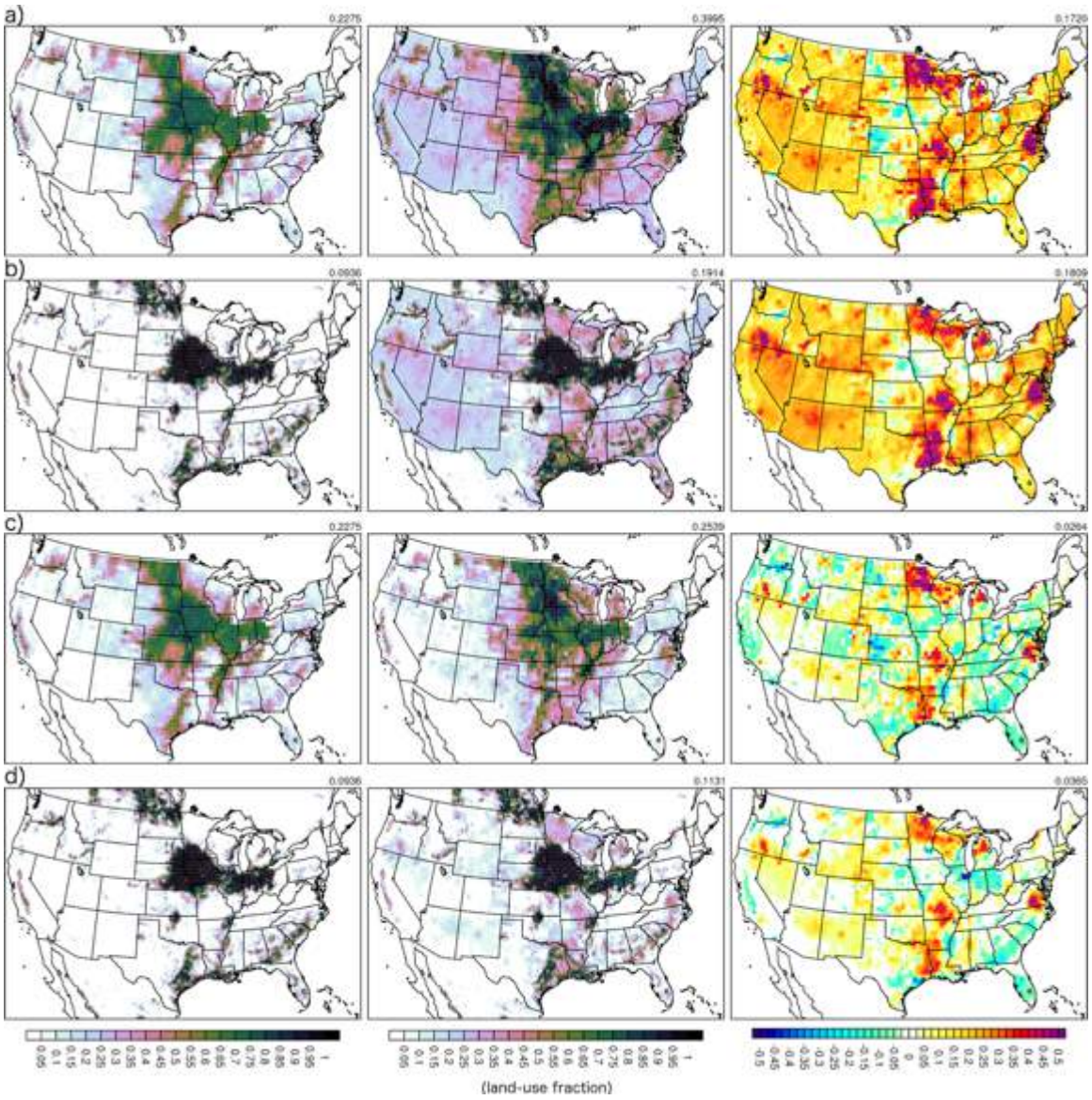

Figure S1. Left column: Historical crop fraction from a) LUM, b) WRF, c) LUM, d) WRF. In WRF, crop fraction is the total of land-use categories 2 and 3. Center column: as in the left column, but for the future crop fraction under a) and b) SSP3LUC, and c) and d) SSP5LUC. Right column: Change in crop fraction from the historical period to the future under a) and b) SSP3LUC, and c) and d) SSP5LUC. Values in the upper right corner of each panel represent the area average for that panel. Note that values outside of the U.S. in WRF have not been masked.

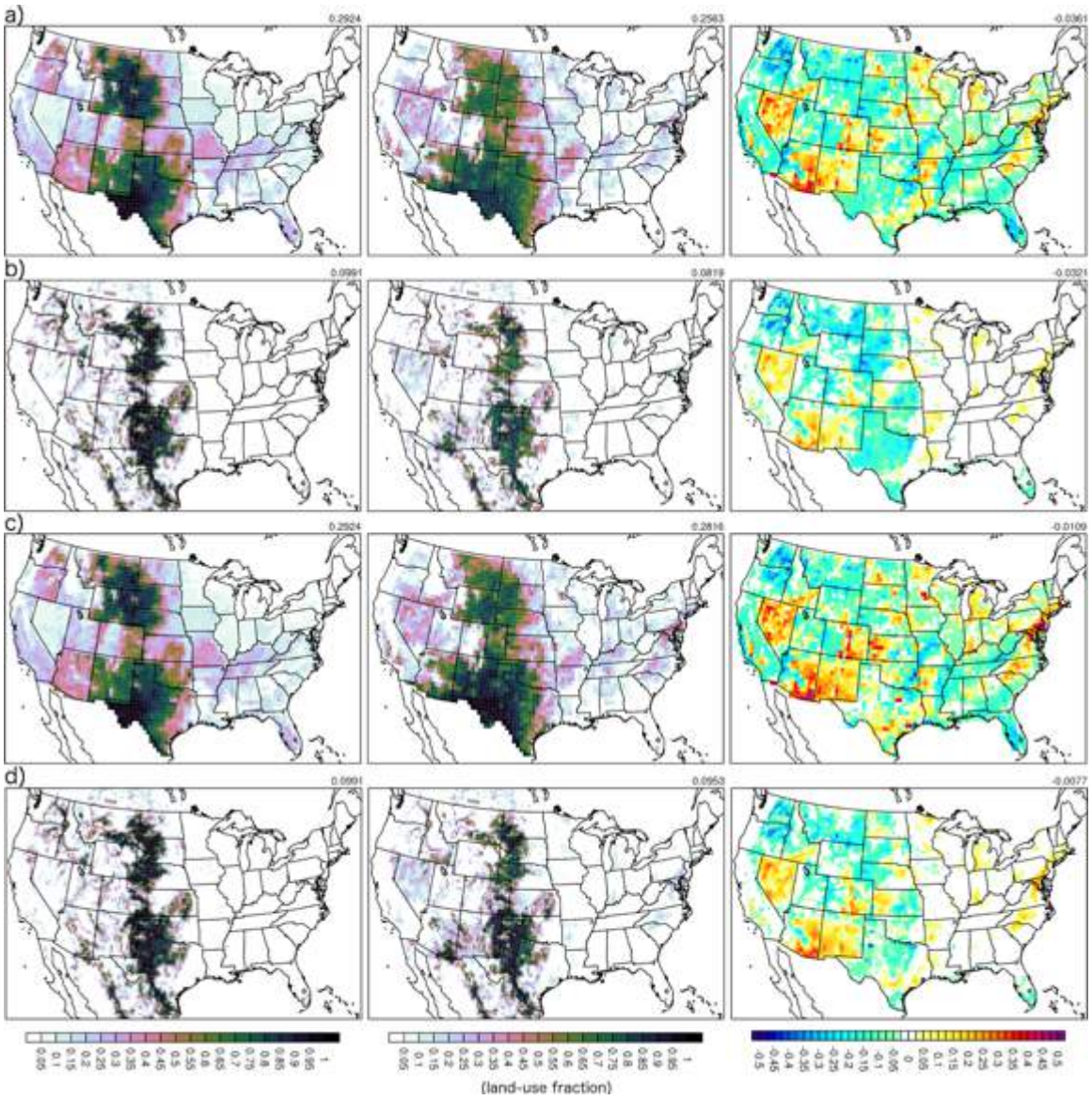

Figure S2. Left column: Historical pasture fraction from a) LUM, b) WRF, c) LUM, d) WRF. In WRF, pasture fraction is represented by land-use category 7. Center column: as in the left column, but for the future pasture fraction under a) and b) SSP3LUC, and c) and d) SSP5LUC. Right column: Change in pasture fraction from the historical period to the future under a) and b) SSP3LUC, and c) and d) SSP5LUC. Values in the upper right corner of each panel represent the area average for that panel. Note that values outside of the U.S. in WRF have not been masked.

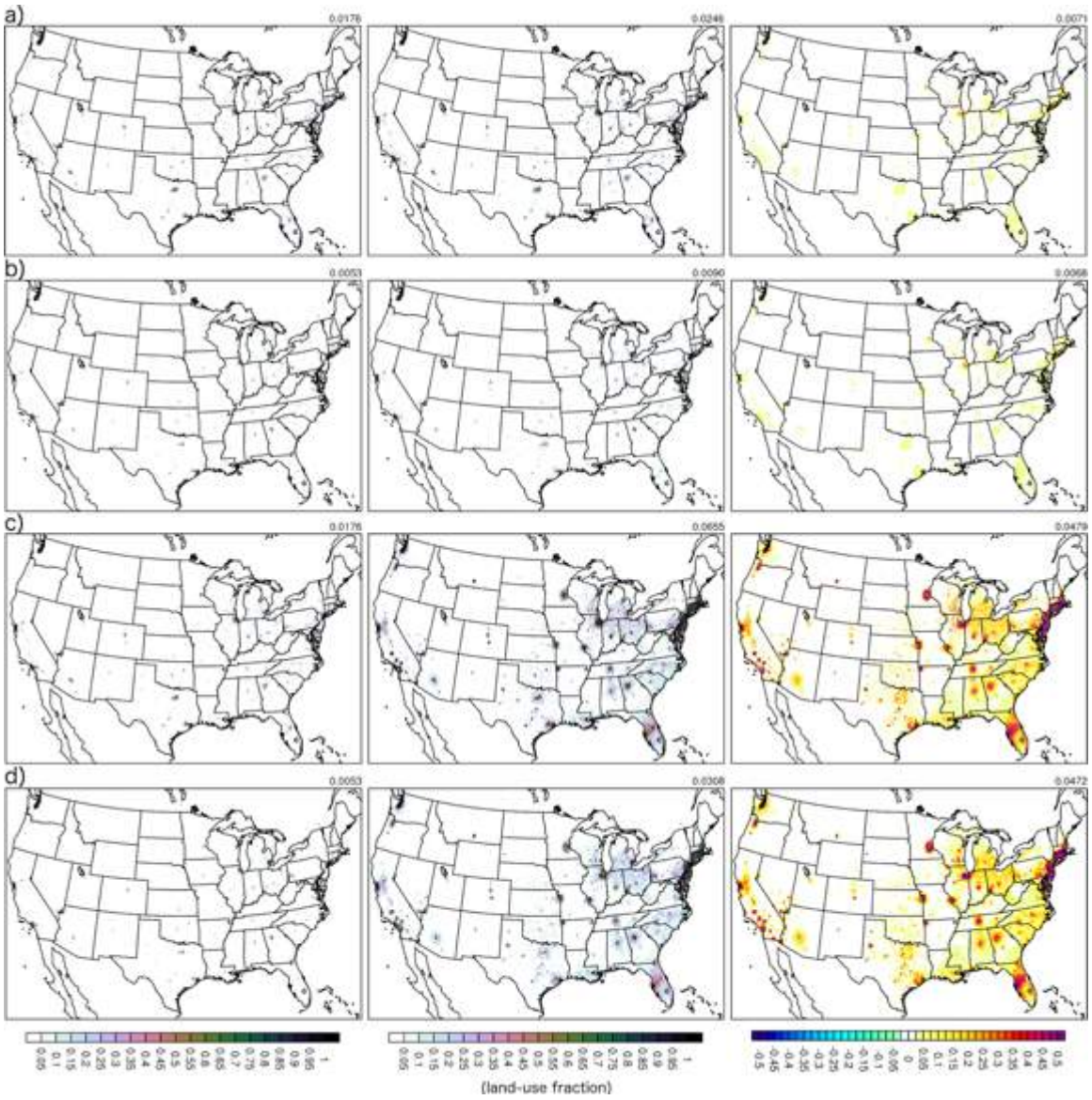

Figure S3. Left column: Historical urban land fraction from a) LUM, b) WRF, c) LUM, d) WRF. In WRF, urban land fraction is represented by land-use category 1. Center column: as in the left column, but for the future urban fraction under a) and b) SSP3LUC, and c) and d) SSP5LUC. Right column: Change in urban land fraction from the historical period to the future under a) and b) SSP3LUC, and c) and d) SSP5LUC. Values in the upper right corner of each panel represent the area average for that panel. Note that values outside of the U.S. in WRF have not been masked.

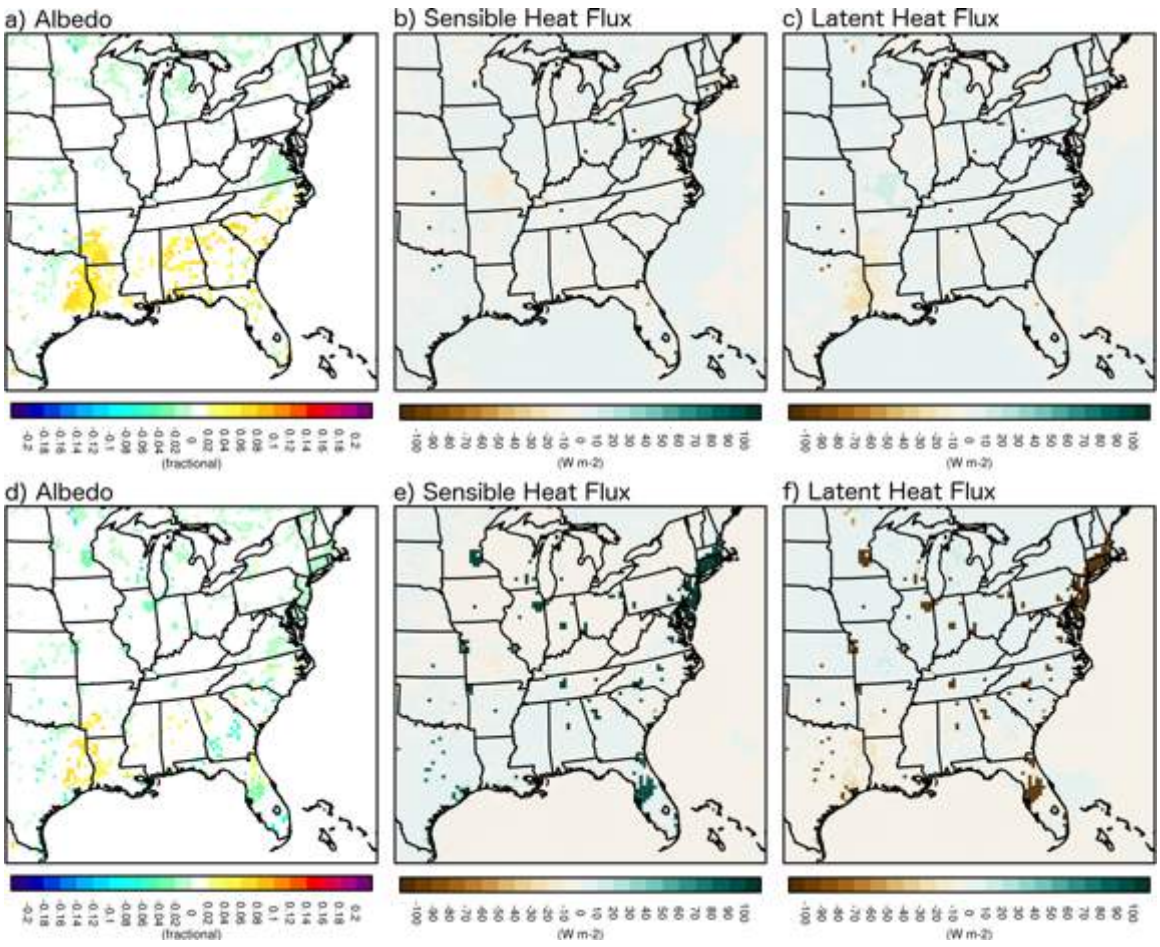

Figure S4. JJA-average absolute difference between projections from the SSP5LUC and noLUC future scenarios for a-c) SSP3LUC-noLUC and d-f) SSP5LUC-noLUC. a) and d) Albedo, b) and e) sensible heat flux, c) and f) latent heat flux.

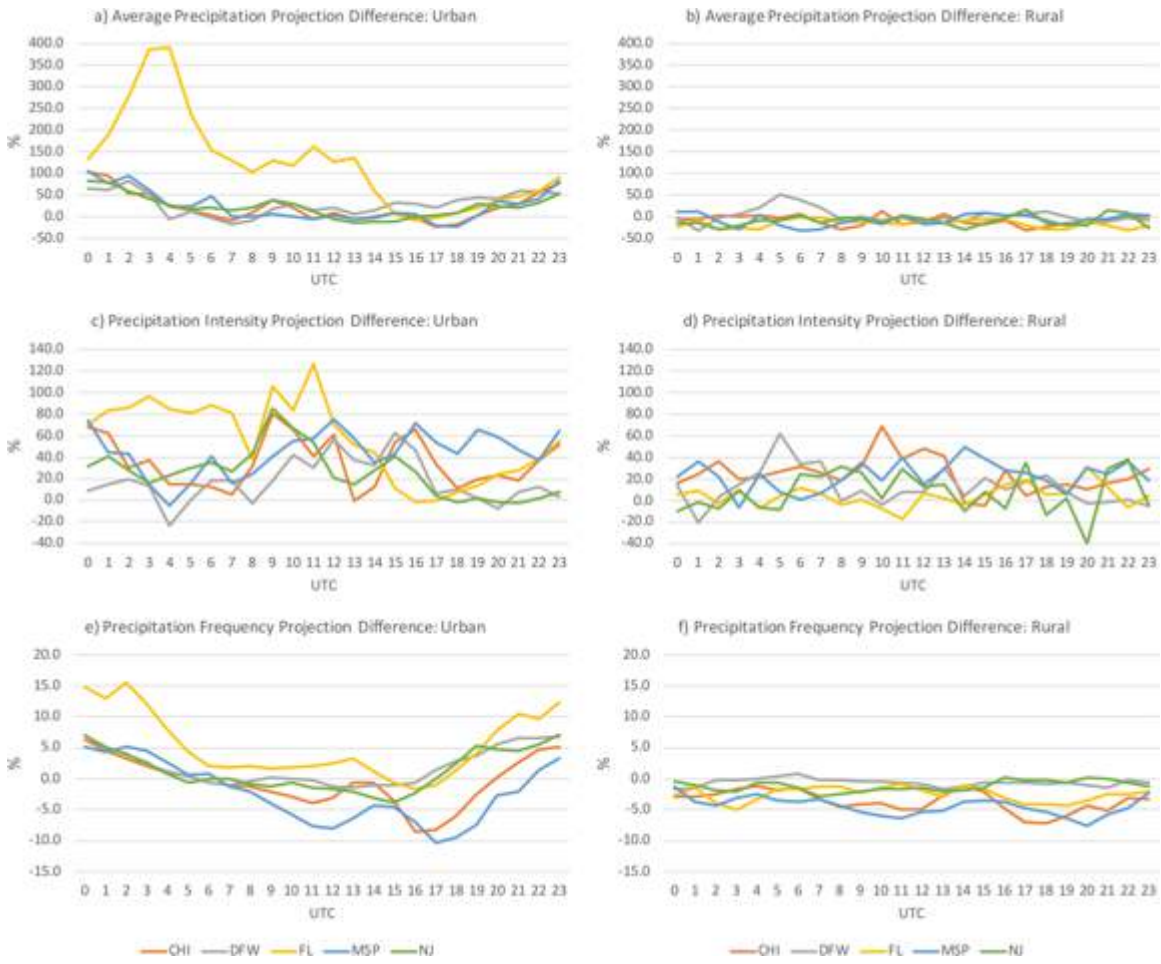

Figure S5. JJA-average absolute difference between projections from the SSP5LUC and noLUC future scenarios for the percent change in a-b) average precipitation, c-d) precipitation intensity, e-f) precipitation frequency, for the full diurnal cycle, using hourly precipitation. The different plot lines reflect the different points indicated in Figure 3 and defined in Section 2.3. a, c, and e) Points that are directly over the urbanization centers, and b, d, and f) eastward/downstream points that are more "rural". Precipitation characteristics are defined in Section 2.4.

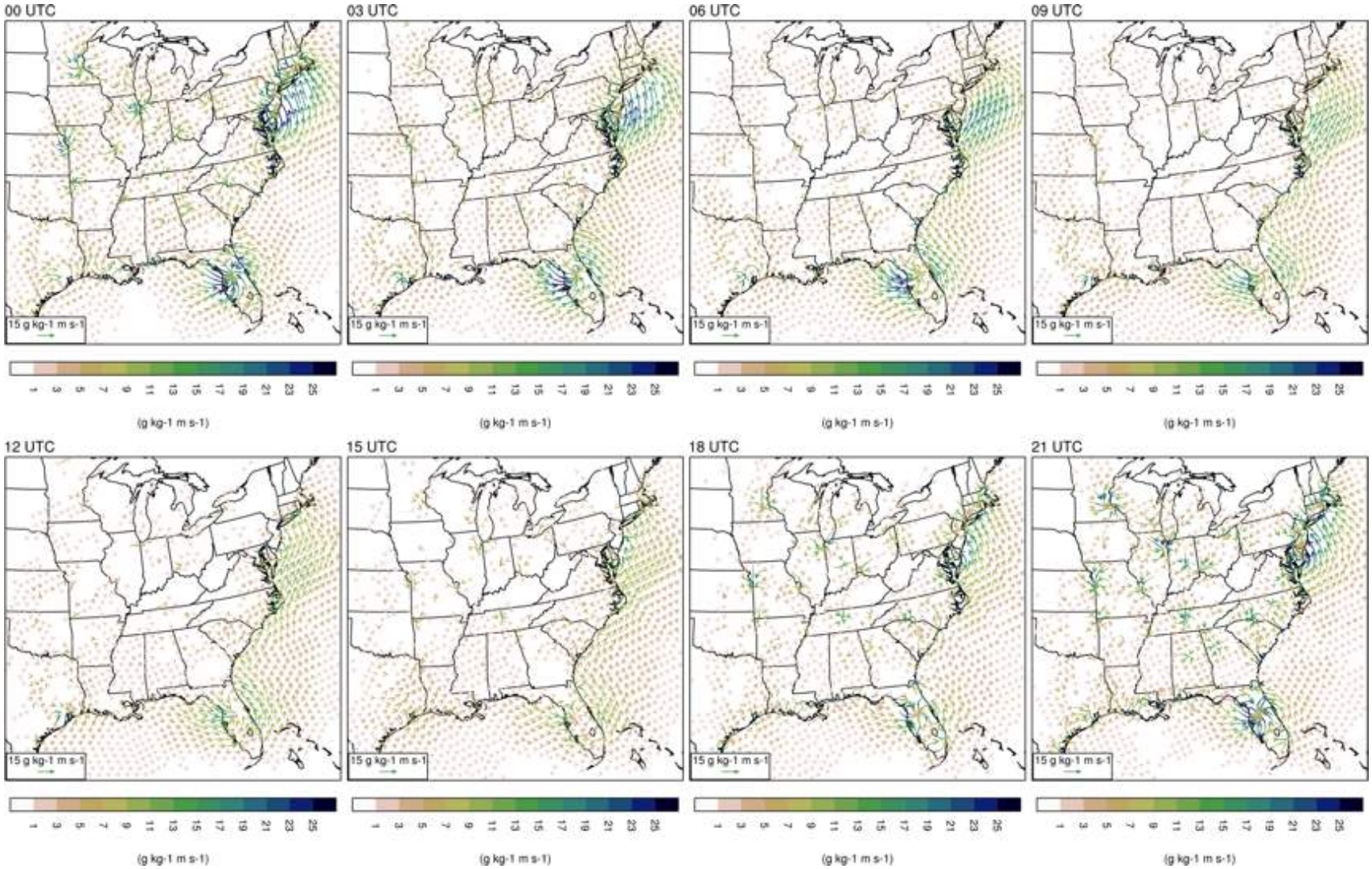

Figure S6. JJA-average absolute difference between projections from the SSP5LUC and noLUC future scenarios for 3-hour average near-surface moisture flux.

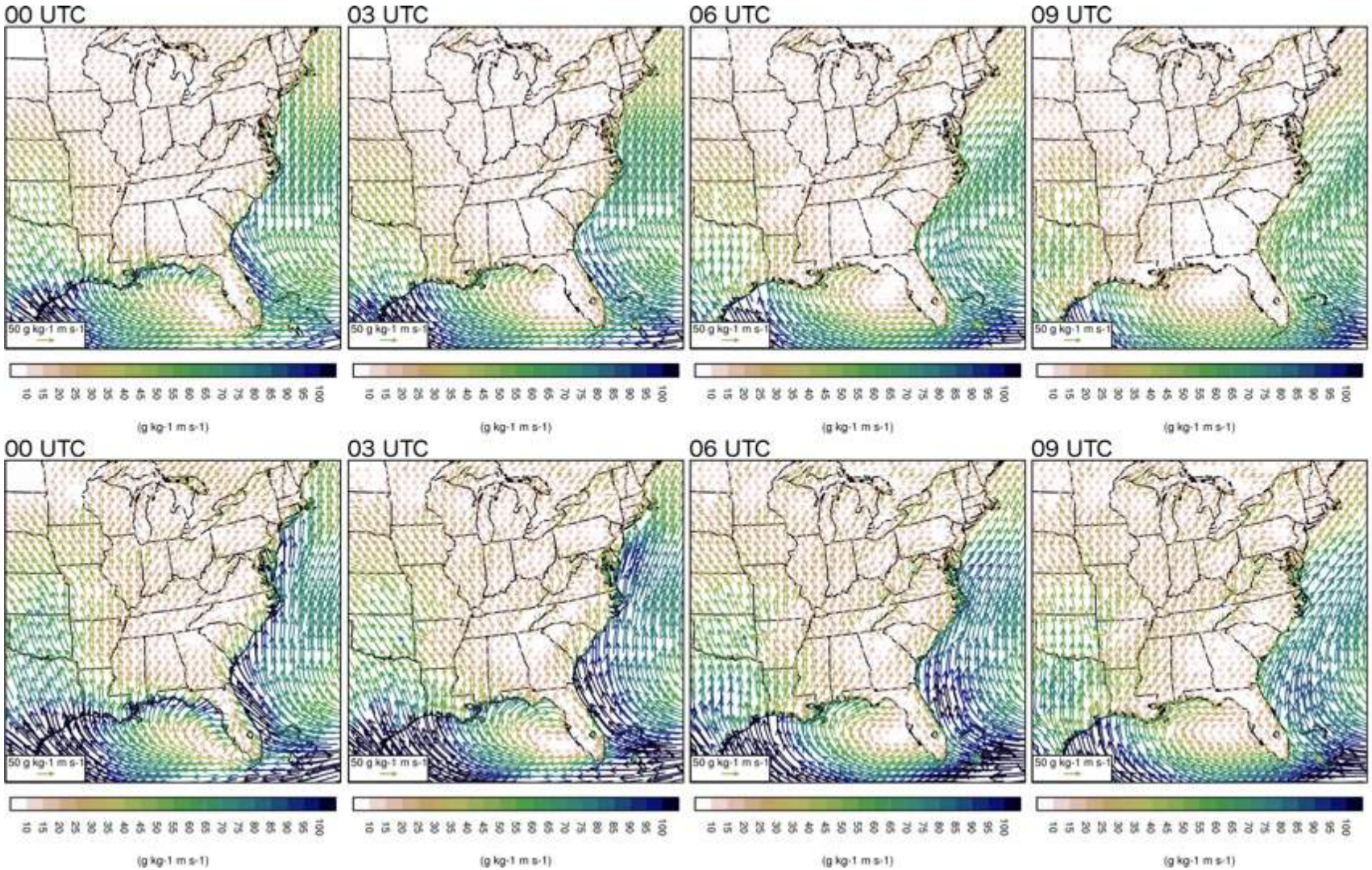

Figure S7a. JJA-average Hist (top row) and SSP5LUC (bottom row) 3-hour average near-surface moisture flux for 00-09 UTC. See Figure 7b for 12-21 UTC.

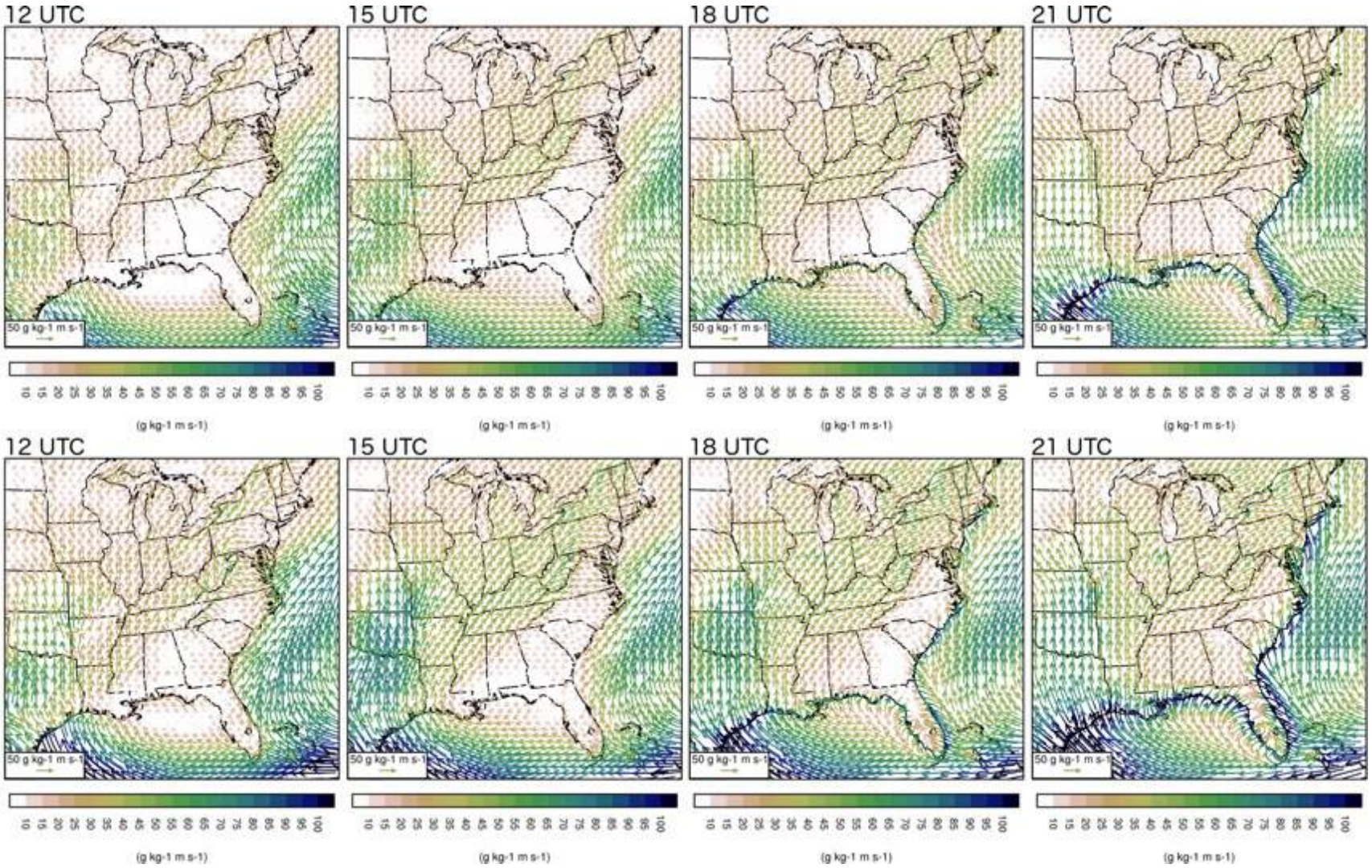

Figure S7b. As in Figure 7a, but for 12-21 UTC.